Mol. Pharm. #MOLPHARM-AR-2020-000184

TITLE PAGE

Cysteine modification by ebselen reduces the stability and cellular levels of 14-3-3 proteins

Kai Waløen, Jung K.C. Kunwar, Elisa D. Vecchia, Sunil Pandey, Norbert Gasparik, Anne Døskeland,

Sudarshan Patil, Rune Kleppe, Jozef Hritz, William H.J. Norton, Aurora Martinez*, and Jan Haavik*

Author Affiliations:

KW, KJKC, SP, AD, SP, AM, & JHa: Department of Biomedicine, University of Bergen, 5009 Bergen,
Norway

EDV & WHJN: Department of Neuroscience, Psychology and Behaviour, College of Medicine,
Biological Sciences and Psychology, University of Leicester, Leicester, LE1 7RH, UK

NG & JHr: CEITEC-MU, Masaryk University, Kamenice 753/5, Bohunice, Brno, Czech Republic

AD: Proteomics Unit (PROBE), Department of Biomedicine, University of Bergen, Bergen, 5009,
Norway

RK: Norwegian Centre for Maritime- and Diving Medicine, Dept. of Occupational Medicine,
Haukeland University Hospital, Bergen, Norway

JHa: Division of psychiatry, Haukeland University Hospital, Bergen, Norway

RUNNING TITLE PAGE

Running title: Ebselen bonding decreases stability of 14-3-3 proteins

*Corresponding author:
JHa, Department of Biomedicine, University of Bergen, 5009 Bergen, Norway
Tel: +47 47235466, +47 55 58 64 32, Fax: +47 - 55 58 63 60, email: jan.haavik@uib.no

*Co-corresponding author:
AM, Department of Biomedicine, University of Bergen, 5009 Bergen, Norway
Tel: +47 55 58 64 27, email: aurora.martinez@uib.no

MANUSCRIPT STATISTICS:

Text pages: 24
Number of tables: 1
Number of figures: 6
Number of references: 62
Number of words in Abstract: 250
Number of words in Introduction: 723
Number of words in Discussion: 1493

Abbreviations: CD, circular dichroism; DSF, differential scanning fluorimetry; DMSO, dimethylsulfoxide; GST, glutathione S-transferase; LC-MS/MS, liquid chromatography-tandem mass spectrometry; MALDI-TOF, matrix-assisted laser desorption/ionization time of flight (MALDI-TOF); SPR, surface plasmon resonance; TH, tyrosine hydroxylase; TPH; tryptophan hydroxylase; WB, western blot

ABSTRACT

The 14-3-3 proteins constitute a family of adapter proteins with many binding partners and biological functions, and are considered promising drug targets in cancer and neuropsychiatry. By screening 1280 small-molecule drugs using differential scanning fluorimetry (DSF), we found 15 compounds that decreased the thermal stability of 14-3-3ζ. Among these compounds, ebselen was identified as a covalent, destabilizing ligand of 14-3-3 isoforms ζ, ε, γ and η. Ebselen bonding decreased 14-3-3ζ binding to its partner Ser19-phosphorylated tyrosine hydroxylase. Characterization of site-directed mutants at cysteine residues in 14-3-3ζ (C25, C94, and C189) by DSF and mass spectroscopy revealed covalent modification by ebselen of all cysteines through a selenylsulphide bond. C25 appeared to be the preferential site of ebselen interaction *in vitro*, whereas modification of C94 was the main determinant for protein destabilization. At therapeutic relevant concentrations ebselen and ebselen-oxide caused a decreased 14-3-3 levels in SHSY5Y, accompanied with an increased degradation, most probably by the ubiquitin-dependent proteasome. Moreover, ebselen-treated zebrafish displayed decreased brain 14-3-3 content, a freezing phenotype and reduced mobility, resembling the effects of lithium, consistent with its proposed action as a safer lithium-mimetic drug. Ebselen has recently emerged as a promising drug candidate in several medical areas, such as cancer, neuropsychiatric disorders and infectious diseases, including Covid-19. Its pleiotropic actions are attributed to antioxidant effects and formation of selenosulfides with critical cysteine residues in proteins. Our work indicates that a destabilization of 14-3-3 may affect the protein interaction networks of this protein family, contributing to the therapeutic potential of ebselen.

SIGNIFICANCE STATEMENT

There is currently great interest in the repurposing of established drugs for new indications and therapeutic targets. This study shows that ebselen, which is a promising drug candidate against cancer, bipolar disorder and the virus infection Covid-19, covalently bonds to cysteine residues in 14-3-3 adaptor proteins, triggering destabilization and increased degradation in cells and intact brain tissue when used in therapeutic concentrations, potentially explaining the behavioral, anti-inflammatory and anti-neoplastic effects of this drug.

Introduction

The 14-3-3 proteins constitute a family of highly conserved acidic proteins that form homo and heterodimers between isoforms. The seven human isoforms of 14-3-3 (β, ε, η, γ, θ, σ, and ζ) are encoded by different genes (Aitken 2006; Yang et al. 2006). Although 14-3-3 proteins have no enzymatic activity, their binding to phosphorylated partners exerts chaperone as well as regulatory functions (van Heusden 2005). As such, 14-3-3 proteins are involved in many vital cellular functions such as transcription, intracellular trafficking, cytoskeletal structure, metabolic regulation and apoptosis (Aitken 2006; Obsil and Obsilova 2011).

Dimers of 14-3-3 protein present an overall W-like shaped structure with the ligand binding grooves facing each other. Each subunit has a characteristic "C" shape and is made up of nine antiparallel α-helices (Figure 1A). The canonical binding site for protein-protein interaction (PPI) in 14-3-3 is situated on the concave surface of each subunit, and binding of a partner protein to 14-3-3 proteins is typically dependent on a phosphorylated Ser or Thr flanked by Arg and Pro residues (Aitken 2006; Obsil and Obsilova 2011).

14-3-3s regulate many cellular processes involved in cancer and neuropsychiatric and metabolic disorders (Hermeking 2003; Pennington et al. 2018; Diallo, Oppong, and Lim 2019; Torrico et al. 2020). Overall, 14-3-3 proteins have >2000 predicted binding partners, and >200 of these have been experimentally identified (Aitken 2006; Pagan et al. 2017; Xiao et al. 2014; Hermeking 2003; Ballone, Centorrino, and Ottmann 2018; Pozuelo Rubio et al. 2004). PPIs are considered a promising field in drug discovery. It has been shown that peptides and derivatives, small molecule compounds and natural products can modulate these PPIs (Stevers et al. 2018). In this context, 14-3-3 proteins are interesting targets due to their large number of binding partners with therapeutic relevance. There are several natural and synthetic stabilizers of 14-3-3 PPIs, such as fusicoccin, cotylenin A, and mizoribine, which originate from fungus, as well as semisynthetic fusicoccin derivatives (Ballone, Centorrino, and Ottmann 2018) and synthetic stabilizers, including molecular tweezers (Bier et al. 2016). On the other hand, some peptides and small molecule compounds, such as R18 and BV02, may function as disruptors of 14-3-3 PPIs (Ballone, Centorrino, and Ottmann 2018). 14-3-3 function also seems to be regulated by oxidation of critical cysteine residues, suggesting additional potential sites for pharmacological intervention (Kim et al. 2014).

Here we report the characterization of a previously unobserved effect of ebselen on 14-3-3 proteins at the molecular, cellular and animal levels. These effects are associated with a covalent interaction with 14-3-3 cysteine residues. Ebselen can interact covalently with cysteine residues in several protein targets (Mukherjee et al. 2014; Favrot et al. 2013; Joice et al. 2013; Lieberman et al. 2014). It

seems to bind to all 14 Cys residues of the nonstructural protein 3 helicase (Mukherjee et al. 2014) but has also been reported to only interact with specific Cys residues in e.g. superoxide dismutase 1 (Capper et al. 2018). Modification of Cys residues by ebselen has been reported to inhibit enzymatic function by forcing conformational changes in target proteins (Favrot et al. 2013; Mukherjee et al. 2014). Ebselen has been proposed as a safe lithium mimetic (Masaki et al. 2016; Singh et al. 2013; Singh et al. 2016) and has been subject to phase II clinical trials for bipolar disorder. Ebselen is also in clinical trials for hearing disorders, diabetes and Covid-19 (https://clinicaltrials.gov/). Out of 10 000 approved drugs and compounds in clinical trials, ebselen showed the strongest inhibition of the main protease (M^{pro}) of SARS-CoV-2 (Jin et al. 2020). Ebselen has also shown activity against other virus protein targets and has been proposed to protect against organ injury caused by Covid-19 (Sies and Parnham 2020; Menendez et al. 2020). Here we show that although all Cys residues in 14-3-3 proteins have the potential to be modified by ebselen, they have different reactivities, and a single residue (C94) is responsible for the protein destabilization observed at low concentrations of ebselen. Ebselen is capable of crossing the blood brain barrier and is pharmacologically active in the brain, making it a compound of interest in drug discovery campaigns related to neurological disorders (Singh et al. 2013). We propose that our findings may provide a foundation for further studies on the repurposing of ebselen and its use as a covalent modulator of 14-3-3 PPI with several therapeutic implications.

MATERIALS AND METHODS

Materials

The Prestwick Chemical Library® from Prestwick Chemical (purchased in 2014) was used for screening. This library consists of 1280 small molecules, of which 95% are approved drugs, at a concentration of 10 mM in 100% DMSO. Ebselen and ebselen oxide were ordered from Sigma Aldrich (Cat# E3520; 2018), except for the experiments in zebrafish, where it was ordered from Cayman Chemical (Cat# 70530; 2018). Active p38-regulated/activated protein kinase (PRAK) was from University of Dundee, MRC PPU Reagents and Services. [32P-γ] ATP was from PerkinElmer (Georgia, USA). Shrimp alkaline phosphatase was from New England Biolabs.

Protein expression, purification and preparation of ebselen-treated 14-3-3ζ

Glutathione S-transferase (GST)- tagged 14-3-3ζ was expressed in *E. coli* (BL21- CodonPlusDE3; Agilent Technologies) (Kleppe et al. 2014). The cells were lysed using French press in PBS buffer, pH 7.4. The GST tagged 14-3-3ζ was immobilized on Glutathione Sepharose 4B (GE Healthcare) and cleaved overnight at 4 °C using 10 U/mL of thrombin (Sigma-Aldrich). The cleaved 14-3-3ζ was collected as flow through. The flow through was filtered using Ultrafree-MC GV centrifugation filters (Merck) and purified further on Superdex 200 increase 10/300 GL (GE Healthcare) gel filtration column using 20 mM HEPES, 200 mM NaCl, pH 7.4. The 14-3-3ζ peak was collected and concentrated using Amicon Ultra 15 mL Centrifugal Filters with a cut-off of 30K (Merck). 14-3-3γ, η and ε were purified as previously reported (Ghorbani et al. 2016; Kleppe et al. 2014). 14-3-3 cysteine mutants were prepared as previously reported (Jandova et al. 2018). TH expression, purification and phosphorylation was performed as reported (Kleppe et al. 2014). Dephosphorylation assay was performed in 15 mM Hepes, 150 mM NaCl, pH 7.4, 10 % glycerol, using TH labelled on Ser19 by PRAK and shrimp alkaline phosphatase essentially as described (Kleppe et al. 2014; Ghorbani et al. 2016), except that no reducing agents were used. Thus, TH (2 mg/ml) was phosphorylated using active p38-regulated/activated protein kinase (PRAK, 7 U/ml) essentially as described (Kleppe et al. 2014, Ghorbani et al. 2016), but in 15 mM Hepes (pH 7.4), 150 mM NaCl, 10 % glycerol without reducing agents, and the PRAK inhibitor epigallocatechin gallate was added (100 µM) after 30 min (25 °C) and pSer19TH kept on ice until used for dephosphorylation. TH (2 µM) with or without 14-3-3 (10 µM) was preincubated on ice for 5 min before starting the dephosphorylation reaction (25 °C) by adding shrimp alkaline phosphatase (0.12 U/µl) and sampling remaining [32P]-labelled TH on phospho-cellulose filters washed in phosphoric acid. Dephosphorylation sample without added phosphatase showed stable level of [32P]-pSer19TH throughout the experiment and was used as 100 %. Except

7

when otherwise indicated, ebselen and ebselen oxide -treated 14-3-3 proteins were prepared by incubating purified 14-3-3 proteins (without any reducing agents) with a 10 fold molar ratio ebselen : 14-3-3 subunits on ice for 30 min, followed by gel filtration to remove excess of compound. Once modified, the T_m-values of the proteins were stable at 4 °C for at least 6 h, and after several cycles of freezing and thawing.

Differential scanning fluorimetry (DSF) and DSF-monitored screening

For DSF-based screening the Agilent Bravo Automated Liquid Handling Platform was used for liquid handling. The final screening volume was 10 μL, with 0.1 mg/mL 14-3-3 in 20 mM HEPES, 200 mM NaCl, pH 7.4, a compound concentration of 400 μM and 4% DMSO, in 384 well plates, with 24 DMSO (4%) controls in each plate. 5X SYPRO Orange (Sigma) was used to monitor protein unfolding in Roche Lightcycler 480. Unfolding curves were recorded with 0.2 °C-intervals with a scan rate of 2 °C/min from 20 to 95°C, with 4 acquisitions per °C including a 10 s hold at 20 °C before and after the experiment, and monitored at λ_{ex} = 465 nm and λ_{em} = 610 nm. The experimental unfolding curves were normalized to fraction of unfolded protein and analyzed to extract the T_m-values for the protein without (DMSO controls) and with compounds (Urbaneja *et al.* 2017). T_m-values (average ± standard deviation (SD)) were calculated for 24 DMSO controls. ΔT_m-values were calculated as the T_m for the protein with compound minus the T_m-value for DMSO control. Any compounds above or below the +/-10xSD (for DMSO control) cutoff value were selected as hits for further validations. The first validation of the initial hits was performed by concentration dependent DSF by measuring 20 points between 0-400 μM and 0-16 μM (n=4). DSF experiments with other 14-3-3 isoforms (γ, η and ε) and 14-3-3ζ mutants were carried out at the same conditions as above. The effect of ebselen on the time dependent unfolding of 14-3-3ζ was measured by monitoring the increase in SYPRO Orange fluorescence, at 37 °C for 17 h, with measurement each 2:17 (min:sec), using the same conditions as for DSF, with 0.1 mg/mL of ebselen-treated and untreated 14-3-3ζ (n=3). The final 14-3-3 protein concentration in these experiments was 0.1 mg/ml (3.7 μM subunit concentration with 2% DMSO in the controls) and the final ebselen concentration was 200 μM (with 2% DMSO).

Circular dichroism (CD)

CD spectra were acquired with a JASCO J-810 spectropolarimeter. CD buffer conditions were 10 mM K_2HPO_4, 150 mM KF, pH 7.4 at 0.2 mg/ml of ebselen-treated (see above) and untreated 14-3-3ζ. Quartz-cuvettes with 0.1 cm path length were used. The samples were measured at 25 °C covering a range of 180-260 nm with a scan rate of 50 nm/min, data pitch of 0.5 nm, response of 0.25 s, sensitivity of 100 mdeg, and 3 accumulations with a band width of 1 nm. The data pitch was 0.2 °C, sensitivity was 100 mdeg with a response of 1 s with a band width of 1 nm. The mean residual

8

ellipticity was determined using the formula $[\theta]mrw = \theta/(n \cdot c \cdot l)$, where θ is the ellipticity (mdeg), c is the protein concentration (M), n is the number of amino acids and l is the path length of the cuvette (cm). Three parallels were averaged after subtraction of baseline spectra and calculation of mean residual ellipticity. Circular dichroism by neural networks (CDNN) (Böhm, Muhr, and Jaenicke 1992) was used to estimate secondary structure content.

Surface plasmon resonance (SPR)

Unless otherwise stated, the method below is the same for all SPR experiments. The Biacore T200 instrument (GE Healthcare Life Sciences) was used. Immobilization of full length 14-3-3ζ (1 mg/ml) was carried out in 10 mM sodium acetate pH 5.1 onto the CM5 sensor chip (GE Healthcare Life Sciences) using standard amine coupling procedure by using PBS as running buffer. The immobilization protocol was 480 s with a flow rate of 7 µl/min followed by 2 h of baseline equilibration. The observed immobilization of about 15 000 response units (RU). The hit compounds were then tested at eight different concentrations between 0-200 µM in running buffer containing 5% DMSO at 25 °C, 30 µL/min flow rate, contact time of 60 s, dissociation time of 200 s, with a final wash after injection with a 50% DMSO solution. The results were analyzed with the Biacore T200 Evaluation software. The binding of pSer19TH to 14-3-3ζ was measured at 25, 50 and 100 nM of the enzyme. The running buffer was PBS with dissociation time of 2000 s, without a final wash step with 50% DMSO solution. The experiments with pSer19TH with ebselen treated 14-3-3ζ were performed with a running buffer of PBS with 5% DMSO, with dissociation time of 2000 s and a final wash step with 50% DMSO solution and solvent correction.

Mass spectrometric LC-MS/MS analysis

20 g of protein pellet from ebselen-treated (see above) and untreated 14-3-3ζ were solubilized and trypsinized at 37 °C overnight. Tryptic peptides were desalted and purified using a reverse-phase Oasis HLB µElution Plate 30 µm (2-mg HLB sorbent, Waters, Milford, MA). After purification of tryptic peptides on Oasis c18 columns, the samples were applied on LC column coupled to Orbitrap Elite in the collision-induced dissociation (CID) and higher energy collisional dissociation (HCD) modes, or on LC column coupled to Orbitrap QExactive. The raw files were analyzed by either Proteome Discoverer software version 2.1.0.81 or Peptide Shaker version 1.16.27 (Vaudel et al. 2015). Three search engines were used MS-Amanda, Sequest and XTandem with a fragment ion mass tolerance of 0.02 Da in HCD mode and 0.6 Da in CID mode and a parent ion tolerance of 10 ppm. Oxidation of methionine and modification of cysteine by ebselen were specified as variable modifications, and a human database was used. Scaffold (version Scaffold_4.8.7, Proteome Software Inc., Portland, OR) was used to validate MS/MS based peptide and protein identifications.

MALDI-MS

The protein samples were incubated with porcine trypsin (Promega) for 2 h at 40 °C in 50 mM ammonium bicarbonate. Matrix-assisted laser desorption/ionization time of flight (MALDI-TOF) mass spectra were obtained using an Ultraflextreme instrument (Bruker Daltonics, Bremen, Germany) operated in linear and reflectron positive ion detection modes for analysis of intact mass of the protein and after proteolysis by trypsin, respectively. The identity of the tryptic peptides was verified by means of MALDI-MS/MS.

Cell culture

SHSY5Y cells (ATCC(r) CRL-2266(tm) (SH-SY5Y); RRID:CVCL0019 from LGC Standards GmbH, Germany), authenticated 8/2019 by short-tandem repeat (STR) DNA profiling and used at maximum 16 passages, were grown in DMEM media with 10% fetal bovine serum, 2 mM glutamine. 1.2×10^6 SHSY5Y cells/p60 plate were seeded and 5 h later cells were treated with 2-20 µM of ebselen or ebselen oxide and DMSO (0.05%) as a control (without ebselen/ebselen oxide). Cells were collected 18 h post-treatment.

Immunofluorescence on SHSY5Y cells

20K SHSY5Y cells/well were seeded on coverslips in 4 well plates and 5 h later were treated with 5 µM ebselen and DMSO (0.05%). Cells were then incubated for 18 h before subjecting to immuno-fluorescence investigation. Cells were fixed with 4% paraformaldehyde for 30 min at RT then permeabilized with PBS 0.2% triton and blocked with 5% FBS in PBS. Primary antibody rabbit anti-pan 14-3-3 (1:100; Santa Cruz) and mouse anti-β-actin (1:100; Sigma) and secondary antibody anti-rabbit alexa fluor 488 (Molecular Probes Cat# A-11008, RRID:AB_143165; 1:200) and anti-mouse alexa fluor 555 (Molecular Probes Cat# A-21422, RRID:AB_141822; 1:200) were used. DAPI (Molecular probes) was used as a nuclear stain. Images were obtained by using Leica microscope TCS SP5 (Leica Microsystem GmbH).

Lysate preparation

Lysates from SHSY5Y cells and zebrafish brain tissues (see below) were prepared in lysis buffer (20 mM HEPES pH 7.0, 10 mM KCl, 1% NP40) containing protease and phosphatase inhibitor. Triton X-100 (1%) was applied to the brain lysates prior to 30 min incubation at 4 °C. Lysates were centrifuged at 10000 rpm for 10 min at 4 °C, supernatant was collected, and protein concentration was measured by using direct detect spectrometer (Merck).

Western blotting (WB)

10

Lysates of SHSY5Y cells or zebrafish brain tissue (5 μg protein) were separated in 10% TGX gels (Bio-Rad) and transferred onto PVDF membrane (Bio-Rad) using the Transblot system (Bio-Rad). WB membranes were incubated with rabbit anti-pan 14-3-3 (Santa Cruz Biotechnology Cat# sc-629, RRID:AB_2273154; 1:1000) as primary antibody. Mouse anti-β-actin (Sigma-Aldrich Cat# A1978, RRID:AB_476692; 1:1000) or rabbit anti-GAPDH (Abcam Cat# ab9485, RRID:AB_307275;1:1000) were used as loading control, and goat anti-rabbit (H+L) (Bio-Rad Cat# 170-6515, RRID:AB_11125142; 1:1000) and goat anti-mouse (H+L) (Bio-Rad Cat# 170-6516, RRID:AB_11125547; 1:1000) as secondary antibodies. Ebselen treated samples were referenced to untreated, which were given the arbitrary value of 1.

For experiments on 14-3-3 degradation in cells, 500K SHSY5Y cells/well were seeded in 6-well plates, 5 h post seeding, cells were treated with 5-10 μM ebselen or ebselen oxide and 50 μM Z-VAD-FMK (caspase inhibitor; Adooq Biosciences) and DMSO (0.05%) as a control (without ebselen and caspase inhibitor). Cells were incubated for 16 h before treating with 500 nM bortezomib (proteasome inhibitor; Fisher Scientific) for 2 h before collecting for Western blot analysis. Densitometric analysis was performed using Image Lab Software 6.0.1 (Bio-Rad).
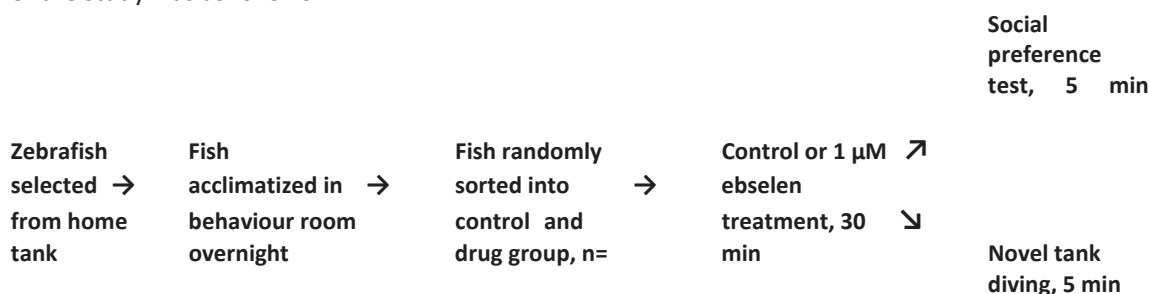
Zebrafish strains, care and maintenance

AB wild-type adult zebrafish (originally from the Zebrafish International Resource Centre; RRID: ZIRC_ZL1) were maintained at the University of Leicester using standard zebrafishkeeping protocols and in accordance with institute guidelines for animal welfare. They were fed twice per day with ZEBRAFEED 400–600 dry food (Sparos). Zebrafish used for behavioural analysis were randomly netted from a large home tank containing approximately 40 fish, and included a mixture of 3 month old male and female AB wild-types. All zebrafish experiments have been approved by the local Animal Welfare and Ethical Review Board (AWERB) and are covered by a UK project licence to Dr Norton, PPL P56FB749.

For experiments with zebrafish brain tissue ebselen was diluted in system water and applied to AB wild-type zebrafish by immersion for 30 min before behavioral testing and for 18 h before dissection for Western blot analysis. Treatment duration and concentrations were chosen according to pilot experiments in our lab. In initial screening experiments, we tested ebselen concentrations between 1- 5 μM to make conditions comparable with cell culture experiments. At 5 μM ebselen, we observed approximately 50% lethality of the zebrafish, while at 1 and 1.5 μM all fish survived during the observation period, without obvious symptoms of distress. In accordance with animal welfare regulations (RRR), we decided to limit the subsequent experiments to a fixed concentration of 1 μM and group sizes of three individuals. At this concentration we observed consistent behavioral effects

11

without any lethality. Three adult zebrafish were used for Western blotting. They were anesthetized with MS222 and sacrificed by decapitation. The brains were quickly dissected in PBS and frozen in liquid nitrogen.

Behavior experiments

All behavioral experiments were carried out between 11:00 and 17:00. Experiments were performed in a dedicated room with light and temperature kept constant. These behavioral experiments are classified as mild on our project license. We minimized any potential suffering by maintaining zebrafish in oxygenated water at the correct temperature of 28 °C during the experimental period. The time-line of the study was as follows:

Zebrafish selected → from home tank	Fish acclimatized in → behaviour room overnight	Fish randomly sorted into → control and drug group, n=	Control or 1 µM ↗ ebselen treatment, 30 ↘ min	Social preference test, 5 min
				Novel tank diving, 5 min

No animals were excluded or died during the behavior experiments.

Visually-mediated social preference for novelty. The social preference for novelty experiment was performed in a transparent rectangular tank composed of five chambers. One central chamber (19 × 13 cm) was surrounded by four identical chambers (9.5 × 6.5 cm). The transparent walls dividing the chambers contained perforated holes to permit water to move between compartments. Social preference test. 3 female adult zebrafish were used as a social stimulus. Their behavior was not included in the data presented here. They were placed in the top left chamber and left to habituate to the novel setting for 5 min. A mixture of ten male and female adult zebrafish were recorded as focal animals. These test fish were placed individually in the central chamber and their behavior was recorded for five minutes from above. The videos were then analyzed to measure time spent swimming and freezing, the primary and secondary endpoints of this study. The zebrafish treated with ebselen were exposed to 1 µM for 30 min. Control zebrafish were immersed in 0.01% DMSO. No exclusion criteria were used in this test, meaning that all animals tested were included in the statistical analysis.

Novel tank test and open field test. Tests were performed in a standard 1.5 L trapezoid tank (Egan et al. 2009) (novel tank test) or a large rectangular arena (43 x 22 x 8 cm). A mixture of ten male and female adult zebrafish were placed individually into the tank and recorded for 5 min. Ethovision software (EthoVision XT, RRID:SCR_000441; Noldus) was used to measure locomotion and the amount of time spent freezing. No exclusion criteria were used in this test, meaning that all animals tested were included in the statistical analysis.

Statistical analysis and study design

Triplicate measurements with different sample preparations were performed and either representative spectra or resulting values as mean ± SD are provided in text or in figure legends. The two-tailed Student's t-test and Welch's two-tailed t-test were used to evaluate significant differences between the samples. For Western blot-based analyses with lysates from neuroblastoma cells and zebrafish, treated samples were referenced to untreated samples, which were given the arbitrary value of 1. All data are presented as mean ± SD of measurements with at least three independent cell culture preparations. Assessment of normality of the data was done using Shapiro-Wilk test. Statistical signification was analyzed by Student's t-test (two-tailed) or one-way ANOVA with the Holm-Sidak method. For the behavioral studies with zebrafish we used 10-12 zebrafish, as indicated, for both the social preference for novelty and novel tank diving assay. This sample size was selected based upon a power analysis using recently reported data (Dalla Vecchia et al. 2019). No blinding was performed. After recording, behaviour was analysed using Ethovision XT tracking software, permitting unbiased comparison of results between treatment groups. All animals were included in the analysis. Zebrafish were then killed using a schedule 1 procedure: overdose of MS222 followed by decapitation as specified by ASPA 1986. Data was first assessed for normality using the Shapiro–Wilk normality test. We did not test for or remove outliers. Statistical analyses were performed using a Mann-Whitney U test or an unpaired Student's t-test with Welch's correction. Statistical analyses were performed using the software GraphPad Prism 8.1.1 (GraphPad Prism, RRID:SCR_002798) and SigmaPlot 13.1 (SigmaPlot, RRID:SCR_003210), and statistical significance was set at $p < 0.05$ for all experiments.

RESULTS

Differential scanning fluorimetry (DSF)-based screening for drugs targeting 14-3-3ζ. Identification of ebselen as a destabilizer that covalently bonds to 14-3-3ζ

To identify compounds capable of binding to 14-3-3ζ, a DSF-based high throughput screen was carried out using an established protocol for identification of binders to protein targets (Niesen, Berglund, and Vedadi 2007; Aubi et al. 2015; Urbaneja et al. 2017). A similar technique has previously been used to identify peptide stabilizers of 14-3-3s (Valenti et al. 2019). The Prestwick Chemical Library (PCL) containing 1280 compounds, 95% of which are approved drugs, was screened. The midpoint melting temperature (T_m) of control samples of 14-3-3ζ with 4% DMSO was 61.1 ± 0.5°C, in agreement with T_m-values previously measured for this protein by thermal dependent CD (Ghosh et al. 2015). Hits were identified based on the change in T_m for the protein (ΔT_m). A $|\Delta T_m| \leq$ (10 x SD (for the DMSO controls)) was selected as the cutoff-value for hit identification. Only destabilizing drugs were identified for 14-3-3ζ and 15 drugs that decreased the T_m of 14-3-3ζ below 56.01 ± 0.5 °C ($|\Delta T_m| \geq 5.1 \pm 0.5$ °C) were selected as primary hits (Figure 1B and Supplemental Table S1). These 15 hits were subjected to detailed concentration dependent DSF analyses at concentrations up to 125 µM. Thimerosal and ebselen showed the most consistent concentration dependent binding curves at these conditions, with large maximal ΔT_m- values -11.6 ± 0.2˚C and -8.1 ± 0.2˚C, respectively; Figure 1B), without inducing 14-3-3ζ denaturation. The organomercury antiseptic compound thimerosal was, however, excluded from further studies on effects on 14-3-3 proteins due to its associated cytotoxicity (Parran, Barker, and Ehrich 2005; James et al. 2005) and ebselen was pursued as the primary hit compound to understand its destabilizing effect and possible interference on partner binding to 14-3-3ζ. The concentration of ebselen that provided a half-maximal decrease in ΔT_m was defined as the $EC_{50,}$, estimated to be 1.50 ± 0.30 (SD) µM for the interaction of ebselen with 14-3-3ζ (Figure 1C). The effects of ebselen on 14-3-3ζ conformation were studied by CD spectroscopy. The CD signal was slightly lower after ebselen treatment (Figure 1D). 14-3-3ζ is a largely α-helical protein (Figure 1A) and, accordingly, the percentage of α-helix calculated using CDNN (Böhm, Muhr, and Jaenicke 1992) for untreated and ebselen treated 14-3-3ζ was approx. 86.4 ± 0.8% and 78.6 ± 1.2%, respectively. These results indicate that the destabilization of the protein caused by ebselen triggers a discrete conformational change of 14-3-3ζ, and is not associated with a large denaturation.

< Fig. 1 >

Ebselen covalently attaches to all cysteine residues in 14-3-3ζ and modification of C94 induces protein destabilization

The interaction between 14-3-3ζ and ebselen was further validated by surface plasmon resonance (SPR). The sensorgram shows that ebselen covalently attaches to the protein and does not dissociate at concentrations up to 25 µM, when a plateau is reached for the response signal quantified in resonance units (RU), suggesting covalent bonding (Figure 2A). Ebselen has previously been shown to modify protein targets mainly through covalent interaction with cysteine residues (Mukherjee et al. 2014; Favrot et al. 2013; Joice et al. 2013; Lieberman et al. 2014). To investigate the possible involvement of cysteines in ebselen-induced destabilization of 14-3-3ζ, we prepared Cys mutants that were analyzed by mass spectroscopy (MS) to identify cysteine residues modified by ebselen treatment of 14-3-3ζ. Using MS/MS with CID detection, we detected ebselen-derivatized by selenylsulphide bonds to tryptic peptides containing either C25, C94 or C189. The identification of a peptide with C94 is illustrated in Figure 2B. Detailed liquid chromatography-tandem MS (LC-MS/MS) and MALDI-TOF MS experiments using the mutants C25A-C189A-14-3-3ζ (Figure 2C and S2A) and C94A-14-3-3ζ (Figure 2D and S2B) contributed to identify C25 as the preferential site of ebselen conjugation with high confidence, followed by C94 and C189. A preferential S-glutathionylation (Kim et al. 2014) and S-nitrosylation (Greco et al. 2006) labelling of C25 in 14-3-3ζ has also been previously reported.

< Fig. 2 >

We also investigated the thermal stability of the Cys mutants by DSF (Table 1). It has been shown that the buried C94 is a determinant for the stability of 14-3-3ζ (Jandova et al. 2018). Accordingly, we noted a protein destabilization caused by mutation of C94, observed in the single mutant C94A and in the double (C25A-C94A and C94A-C189A) and triple mutants, which presented a decrease in T_m of 3.2-5.9 °C compared with wild-type (WT)-14-3-3ζ (Table 1). On the other hand, mutations at C25 and C189 did not affect the protein stability, as seen with the C25A and C25A-C189A mutants (Table 1). With respect to the ebselen effect, both triple mutants (C25A-C94I-C189A and C25A-C94V-C189A) were unaffected by ebselen treatment, which excluded the possibility that the destabilization originated from modification of 14-3-3ζ at other residues than cysteine. The results also indicate that ebselen induced only minor changes in T_m in C94-mutants, while the two mutants at other residues

15

but with C94 intact (C25A and C25A-C189A) showed a similar destabilization (8.6-9.0 °C decrease in T_m) as WT-14-3-3ζ (Table 1), pointing to C94 as the site for ebselenation-mediated destabilization.

Altogether, the MS analyses of 14-3-3ζ and Cys mutants revealed a complex pattern of Cys modification by ebselen, which appeared to occur at all Cys residues, to a larger degree for C25 and lesser extent for C94 and C189, whereas the DSF assays of mutated proteins (Table 1) indicate that the destabilization is dependent on the ebselen-modification of C94.

< Table 1 >

Ebselen modification of 14-3-3ζ affects its kinetic stability and its interaction with TH phosphorylated at Ser19 (pSer19-TH)

Based on the discrete destabilization of 14-3-3ζ observed by ebselen treatment, leading to an approx. 7 °C reduction in T_m (see above and Table 1), it is not straightforward to predict subsequent physiological consequences of ebselen modification. By measuring the fluorescence-monitored isothermal loss of conformational stability of the protein at 37 °C we observed a several fold-increased rate of unfolding for the ebselen-treated 14-3-3ζ compared with the untreated control (Fig. 3A). This indicates that the protein may show altered stability also at physiological conditions. The functional consequences of the destabilizing conformational change of 14-3-3ζ was explored by examining its interaction with a physiologically relevant protein partner. To this end, we measured the binding of the archetypical 14-3-3 partner Ser19-phosphorylated TH (pSer19TH) to ebselen-treated and untreated 14-3-3ζ by SPR. Complex formation of pSer19TH with 14-3-3 proteins is of high affinity, and activates and stabilizes TH (Ghorbani et al. 2016). As seen in Figure 3B, the binding of ebselen treated 14-3-3ζ to pSer19TH was reduced compared to the untreated protein.

Ebselen destabilizes several 14-3-3 isoforms

We further investigated if the destabilizing effect of ebselen on 14-3-3ζ could also be observed for other 14-3-3 isoforms. All these proteins have conserved Cys residues at positions equivalent to C94 in the ζ isoform; C189 is conserved in all isoforms except in σ and C25 is not conserved (Figure S1). 14-3-3η showed the lowest thermal stability (T_m = 47.9 ± 0.2 °C), followed by 14-3-3γ (56.9 ± 0.2 °C), while 14-3-3ε (59.7 ± 0.1 °C) and 14-3-3ζ (59.9 ± 0.3 °C) had similar T_m-values (Table 1). All tested

16

isoforms were destabilized by ebselen, however, in contrast to 14-3-3ζ, ebselen treatment did not elicit a discrete destabilizing conformational change in these isoforms, but rather a major destabilization, as observed for the ε and γ isoforms, or denaturation for η (Figure 3C, Table 1 and data not shown). Curiously, a concentration effect threshold was seen at low concentrations of ebselen in the concentration dependent destabilization (ΔT_m-values) for 14-3-3 ζ (Figure 3C), which was not observed in the other tested isoforms, and 14-3-3ζ was also the most resilient isoform against the destabilizing effects of ebselen. The apparent concentration threshold of 14-3-3ζ modification may indicate that an intact C25 exerts a stabilizing effect on this protein. Only when C25 has been modified, the consecutive bonding of ebselen to C94 would lead to destabilization of the ζ isoform.

We have reported that the interaction between pSer19TH and 14-3-3 is conserved between different isoforms, but that 14-3-3γ had the strongest effect on activation and inhibition of pSer19TH dephosphorylation (Ghorbani et al. 2016). 14-3-3 proteins also modulated access to other regulatory sites for multi-site phosphorylation of TH (Ghorbani et al. 2020). As inhibition of TH dephosphorylation is a sensitive functional readout of 14-3-3, we conducted dephosphorylation experiments with [^{32}P]-labelled pSer19TH in the presence or absence of 14-3-3γ, or 14-3-3γ pre-treated with ebselen or ebselen oxide (Fig. 3D). PRAK phosphorylated TH (pSer19TH) was stably labeled throughout the dephosphorylation experiment as shown in absence of added phosphatase (Fig. 3D) and was rapidly dephosphorylated in the absence of unmodified 14-3-3γ, which inhibited dephosphorylation substantially. This was however not the case for ebselen treated 14-3-3, which showed no significant inhibition compared to no 14-3-3, whereas ebselen oxide treated 14-3-3 showed some residual inhibition (Fig. 3D).

In conclusion, it appears that 14-3-3 isoforms behave differently in the presence of ebselen, and these differences can be hypothesized to be due to differences in cysteine residues within the protein.

< Fig. 3 >

Ebselen treatment of SHSY5Y cells triggers proteasomal degradation of 14-3-3

To test the effects of ebselen on 14-3-3 protein stability and turnover in intact cells, we performed immunofluorescence imaging of SHSY5Y cells treated with ebselen. After evaluating the viability of

17

the cells at different ebselen and DMSO concentrations, 5 µM ebselen with 0.05% DMSO was selected, using untreated as well as a DMSO-control (0.05%) cells for comparison (Figure 4A). The levels of DAPI, 14-3-3, and β-actin were virtually unchanged for the untreated and DMSO control cells. However, the 14-3-3 signal was significantly reduced in cells treated with ebselen. This was confirmed by Western blotting experiments and densitometric analysis, showing that ebselen-treated cells had 28 ± 13% decreased 14-3-3 levels compared to untreated cells (Figure 4B). To investigate the mechanism for 14-3-3 depletion, cells were treated with ebselen, a proteasome inhibitor (Bortezomib), and a caspase inhibitor (Z-VAD-FMK). Cell samples pretreated with ebselen, and then treated with either the proteasomal inhibitor or a mixture of proteasomal and caspase inhibitors, showed a significant increase in 14-3-3 level compared to cell samples only treated with ebselen. However, samples treated with ebselen and then with the caspase inhibitor showed similar level of 14-3-3 as the samples treated only with ebselen. These results indicate that ebselen treatment triggers a proteasome-mediated degradation of 14-3-3 in SHSY5Y cells (Figure 4C).

< Fig. 4 >

Comparison of ebselen and ebselen oxide

Previous studies have shown that ebselen can act as an antioxidant and reduce hydroperoxides. During this process, ebselen is converted into the antioxidant inactive derivative ebselen oxide (Lass et al. 1996). To explore whether the cellular effects of ebselen might be mediated by its oxidized derivative, we compared the effects of ebselen and ebselen oxide. As shown in Fig. 5, ebselen and ebselen oxide had slightly different effects on the viability of SHSY5Y cells (Supplementary Figure S3). At 20 µM ebselen oxide, the cellular viability was reduced by 71 %, compared to 41 % reduced viability by ebselen at this concentration (P= 0.007, for comparison, t-test). However, the effects of ebselen and ebselen oxide on cellular levels of 14-3-3 were rather similar, as reported for other protein targets (Wang et al. 2017). For both compounds, the levels of 14-3-3s gradually decreased at concentrations exceeding 2 µM and the effects were abolished by treatment with bortezomib. A similar decrease of 14-3-3 levels was observed using either14-3-3ζ specific antibodies or pan-14-3-3 antibodies, suggesting that the decrease was not limited to one particular isoform. Based on these studies, we conclude that the observed effects of ebselen on intact cells could (partially) be mediated by its oxidized derivative(s).

< Fig. 5 >

In vivo action of ebselen in zebrafish brain

The effect of ebselen on 14-3-3 proteins was also studied in adult zebrafish. Zebrafish were treated with 1 µM ebselen for 18 h before the brains were collected. Western blot was performed using the brain lysates of ebselen treated zebrafish vs untreated (DMSO control). Densitometric analysis showed a significant reduction of 14-3-3 in the brain of zebrafish treated with ebselen, compared to untreated control (Figure 6A). This reduction in 14-3-3 abundance was in accordance with our observation in SHSY5Y cells (Figure 4).

A visually mediated social preference test was carried out following treatment with 1 µM ebselen for 30 min (n = 30) (Figure 6B) (Carreño Gutiérrez et al. 2019). Zebrafish immersed in 0.01% DMSO control water froze for approximately 25 s. In comparison, zebrafish treated with 1 µM ebselen froze for more than 100 s (Figure 6C). Moreover, zebrafish treated with DMSO swam for approximately 1250 cm, whereas the ebselen treated zebrafish only swam about 500 cm (Figure 6D). The novel tank test (Figure 6E) and the open field test (Figure 6H) were also carried out. These tests revealed no significant differences between DMSO and ebselen treated zebrafish in terms of time spent frozen and distance travelled (Figure 6F,G,I,J). This is similar to previous research reporting that zebrafish treated with lithium display approximately half the mobility of untreated zebrafish (Nery et al. 2014). The lithium effect has been associated to direct binding and inhibition of targets such as glycogen synthase kinase 3ß (GSK3B) and inositol monophosphatase (IMPase). Interestingly, IMPase is also efficiently inhibited by ebselen (Singh et al. 2013; Masaki et al. 2016; Singh et al. 2016). To explore this connection, we used a DSF-monitored binding assay to investigate whether lithium would directly bind to 14-3-3ζ. However, no apparent binding was observed when lithium tested in the concentration range 0.01 µM to 10 mM (data not shown).

< Fig. 6 >

DISCUSSION

In this work, we screened a chemical library to find compounds that interact with 14-3-3ζ. This isoform was selected for initial screening due to its high abundance in the CNS and strong involvement in human physiological functions and disorders (Torrico et al. 2020). Strikingly, only destabilizing compounds were found. This is unusual for DSF-based screens, which customarily result in identification of both stabilizing and destabilizing ligands (Niesen, Berglund, and Vedadi 2007; Aubi et al. 2015). The 14-3-3 destabilizing drugs belong to different therapeutic classes, with an overrepresentation of proton pump inhibitors and calcium channel blockers, several of them including S or Se in their structure (Table S1). Ebselen was identified as a destabilizer through covalent bonding to 14-3-3ζ, bonds, and similarly shown to modify and destabilize 14-3-3ε, γ and η, but with markedly large differences between these highly conserved isoforms.

Ebselen is a synthetic seleno-organic compound with several biological activities including anti-oxidant, anti-inflammatory, and glutathione peroxidase mimicking activity (Azad and Tomar 2014). (Lass et al. 1996). Ebselen has previously been shown to modify protein function through covalent bonding with cysteine residues via its Se atom, forming stable selenenylsulfide (–Se–S–) bonds (Favrot et al. 2013; Mukherjee et al. 2014), as confirmed also here by LC-MS/MS for the formation of ebselenated adducts of the modified Cys residues in 14-3-3ζ. Ebselen destabilized 14-3-3ζ, which contains three Cys residues, C25, C94 and C189 (Figure 1A and Supplemental Figure S1). We calculated the solvent accessibility of all three Cys residues in 14-3-3ζ using the program Getarea (http://curie.utmb.edu/getarea.html) and all previously published 3D structures of this isoform (PDB IDs 1QJA, 1QJB, 2C1N, 2O02, 4FJ3, 5D2D, 5EXA, 5NAS, 6F08, and 6FNA, with ligands removed). This analysis showed that C25 and C189 are partially solvent accessible, 2.6-13.8% (average 7.04%) and 17.6-30.4% (Average 25.17%), in different structures respectively, whereas C94 was found to be solvent inaccessible in all structures. Thus, a priori, C25 and C189 would appear to be preferred targets for ebselen modification. However, previous studies have shown that ebselen is also capable of covalently modifying deeply embedded Cys residues (Mukherjee et al. 2014).

A concentration effect-threshold was observed at the lowest concentrations in the concentration dependent DSF screen of 14-3-3ζ, most probably explained by the stabilizing effect of C25, which is not present in isoforms ε, γ or η (Supplemental Fig. S1), whereas destabilization appears associated to ebselen modification of C94. Protein destabilization brought about by conformational changes has been previously shown as an effective mechanism of drug action (Ren et al. 2018). In the case of the ebselenated Mycobacterium tuberculosis antigen 85 (*Mtb* Ag85) complex, it has been shown that ebselen bonding triggers structural changes accompanied by a decrease in protein thermal stability

20

(Goins et al. 2017). Thus, the CD results corroborate the destabilizing effect of ebselen due to a discrete conformational effect on 14-3-3ζ without denaturing the protein, even after treatment with a high and saturating concentration of ebselen (200 μM).

The functional consequences of the destabilizing conformational change of 14-3-3ζ were demonstrated by showing a decreased interaction with the physiologically relevant protein partner TH. Together with the tryptophan hydroxylases (TPHs) 1 and 2, TH was amongst the first proteins identified to bind to 14-3-3's (Ichimura et al. 1987). The interaction between 14-3-3 proteins and TH primarily takes place at phosphorylated Ser19 on the N terminal tail of TH. This phosphorylated amino acid interacts with two conserved Arg and one Tyr residue of 14-3-3 within the main binding cleft (PDB 4J6S) (Skjevik et al. 2014). TH catalyzes the rate-limiting step in the biosynthesis of dopamine. Thus, compounds that modulate the TH:14-3-3 interaction could represent potential therapeutics for disorders related to altered dopamine function, such as attention deficit hyperactive disorder, parkinsonism, and Parkinson's disease (Del Campo et al. 2011; Waloen et al. 2017). Similarly, the 14-3-3 regulated enzymes TPH1 and TPH2 catalyze the rate limiting reaction in the synthesis of serotonin, an important signaling molecule, and these TPH:14-3-3 complexes also represent relevant therapeutic targets (Waloen et al. 2017).

We also explored how ebselen treatment influenced 14-3-3 levels in intact cells and tissues. Increased protein instability caused by mutations or chemical modifications usually results in dysfunction and reduction of cellular protein levels due to increased processing of the proteins by quality control systems, notably through the ubiquitin-dependent proteasome system (Vilchez, Saez, and Dillin 2014). Caspase-dependent degradation has been reported to be implicated in the reduction of 14-3-3ζ levels following intracellular oxidation (Kim et al. 2014). On the other hand proteasome-mediated 14-3-3 degradation of the γ isoform has also been reported (Chen et al. 2015).

The function and regulation of 14-3-3 proteins have been studied in several cell types derived from the nervous system, notably the SHSY5Y neuroblastoma cell line. These cells express multiple 14-3-3 isoforms, including 14-3-3 ε and ζ that were of particular interest in our study. It was recently shown that these 14-3-3 isoforms are subject to ubiquitin regulated proteasomal degradation in SHSY5Y cells (Jiang et al. 2019). Our observation that ebselen treatment triggered ubiquitin-mediated proteasomal degradation of 14-3-3s in SHSY5Y cells (Fig. 4C) is consistent with these findings.

Proteasome-mediated degradation of ebselen, and ebselen oxide modified proteins has previously been reported (Li et al). It nevertheless possible, that the effect of ebselen on 14-3-3 levels may be indirect, by i.e. increasing the phosphorylation, ubiquitination, or other covalent modification of 14-

21

3-3s, as such modifications are reported to trigger 14-3-3 degradation (Jiang et al. 2019; Chen et al. 2015).

14-3-3 proteins constitute approx. 1% of total soluble brain proteins (Aitken 2006). They are involved in multiple functions, including metabolic regulation and cortical development (Cornell and Toyo-Oka 2017). Common and rare genetic variants in 14-3-3s are implicated in multiple neuropsychiatric disorders, making the 14-3-3s and their protein-partner networks attractive as therapeutic targets in neuropsychiatry (Pagan et al. 2017; Jacobsen et al. 2015; Torrico et al. 2020). The *in* vivo experiments showed that zebrafish treated with ebselen exhibited a freezing behavior and reduced locomotion (Fig. 6). Similarly, ebselen reduces impulsivity in rodent models and has been suggested as an alternative to lithium in the treatment of bipolar disorder and other mood disorders (Singh et al. 2013; Singh et al. 2016). Lithium has severe side effects, whereas ebselen has limited toxicity at brain-active therapeutic concentrations, which makes ebselen a potential safer treatment alternative (Singh et al. 2013; Singh et al. 2016). 14-3-3s regulates the established lithium target GSK3B (Liao et al. 2005; Sugden et al. 2008), pointing to crosstalk of protein networks targeted by lithium and by alteration of 14-3-3 functionality. This indicates that alteration of protein interaction networks involving 14-3-3s may contribute to the lithium-mimicking effect of ebselen. Nevertheless, elucidation of the molecular basis for the phenotype caused by ebselen treatment requires further investigation. Moreover, due to the broad and rather non-specific effects of ebselen it is very probable that other molecular targets also are involved in its lithium-mimicking activity. Interestingly, we did not observe any direct binding of lithium to 14-3-3ζ at therapeutically relevant concentrations.

Overexpression of 14-3-3 has been found in several cancer forms and is associated with poor prognosis and aggressive tumor growth (Xiao et al. 2014; Liu et al. 2014). Reduction of 14-3-3 abundance makes cancer cells more susceptible to chemotherapy treatment, and 14-3-3s are considered attractive targets for cancer therapy (Cao et al. 2015; Woodcock et al. 2015). Thus, the ebselen effect on 14-3-3 turnover and consequent alteration of the PPI network is also expected to be relevant for cancer treatment. Actually, cysteine residues in 14-3-3 are targets of photodynamic light cancer therapy mediated by reactive oxygen species, where oxidization of these residues is expected to mediate the apoptosis triggered by such treatment (Helander et al. 2016). Our work, showing the ability of ebselen to reduce the abundance and function of 14-3-3 *in vivo* through cysteine modification, also reinforces the promise of ebselen as an exciting candidate to use in cancer treatment in addition to mood disorders. Furthermore, this study also identified 15 other small-molecule drugs with destabilizing effects on 14-3-3ζ (Table S1). These compounds share redox

activity properties with ebselen, and include S atoms, indicating that their destabilizing effects on 14-3-3s may also be mediated by interaction with cysteine residues. As ebselen is a redox active compound, its effects may be modified in cells and in vivo by glutathione, free cysteine or other cellular sulfhydryl compounds, by reducing the selenylsulphide bonds.

In summary, the destabilizing effect of ebselen binding to 14-3-3 proteins suggest that disruption of 14-3-3 protein interactions may contribute to the biological effects of ebselen in cancer, neuropsychiatric and infectious disorders. Moreover, ebselen has recently also been proposed as a treatment of Covid-19 and other respiratory viral infections (Sies and Parnham 2020). Here we show that ebselen bonding has some specificity and has differential effects also within the highly conserved group of 14-3-3 proteins. However, even more selective binding to specific Cys residues in protein targets may be necessary to achieve the specificity required for further clinical applications of this drug.

ACKNOWLEDGEMENTS

AUTHORSHIP CONTRIBUTIONS

AM, JHa (Bergen), WN (Leicester) and JH (Brno) managed and designed research. KW, KJKC, EDV, SP, AD, and NG conducted the experiments and analyzed the results. KW, AM and JH (Bergen) wrote the paper and all authors revised, edited, read and accepted the manuscript.

REFERENCES

Aitken, A. 2006. '14-3-3 proteins: A historic overview', *Seminars in Cancer Biology*, 16: 162-72.

Aubi, O., M. I. Flydal, H. Zheng, L. Skjaerven, I. Rekand, H. K. Leiros, B. E. Haug, N. P. Cianciotto, A. Martinez, and J. Underhaug. 2015. 'Discovery of a Specific Inhibitor of Pyomelanin Synthesis in Legionella pneumophila', *J Med Chem*, 58: 8402-12.

Azad, G. K., and R. S. Tomar. 2014. 'Ebselen, a promising antioxidant drug: mechanisms of action and targets of biological pathways', *Mol Biol Rep*, 41: 4865-79.

Ballone, A., F. Centorrino, and C. Ottmann. 2018. '14-3-3: A Case Study in PPI Modulation', *Molecules*, 23.

Bier, D., M. Bartel, K. Sies, S. Halbach, Y. Higuchi, Y. Haranosono, T. Brummer, N. Kato, and C. Ottmann. 2016. 'Small-Molecule Stabilization of the 14-3-3/Gab2 Protein-Protein Interaction (PPI) Interface', *Chemmedchem*, 11: 911-18.

Böhm, G., R. Muhr, and R. Jaenicke. 1992. 'Quantitative analysis of protein far UV circular dichroism spectra by neural networks', *Protein Eng*, 5: 191-5.

Cao, L., H. Lei, M. Z. Chang, Z. Q. Liu, and X. H. Bie. 2015. 'Down-regulation of 14-3-3beta exerts anti-cancer effects through inducing ER stress in human glioma U87 cells: Involvement of CHOP-Wnt pathway', *Biochem Biophys Res Commun*, 462: 389-95.

Capper, M. J., G. S. A. Wright, L. Barbieri, E. Luchinat, E. Mercatelli, L. McAlary, J. J. Yerbury, P. M. O'Neill, S. V. Antonyuk, L. Banci, and S. S. Hasnain. 2018. 'The cysteine-reactive small molecule ebselen facilitates effective SOD1 maturation', *Nat Commun*, 9: 1693.

Carreño Gutiérrez, H., S. Colanesi, B. Cooper, F. Reichmann, A. M. J. Young, R. N. Kelsh, and W. H. J. Norton. 2019. 'Endothelin neurotransmitter signalling controls zebrafish social behaviour', *Sci Rep*, 9: 3040.

Chen, D. Y., D. F. Dai, Y. Hua, and W. Q. Qi. 2015. 'p53 suppresses 14-3-3γ by stimulating proteasome-mediated 14-3-3γ protein degradation', *Int J Oncol*, 46: 818-24.

Cornell, B., and K. Toyo-Oka. 2017. '14-3-3 Proteins in Brain Development: Neurogenesis, Neuronal Migration and Neuromorphogenesis', *Front Mol Neurosci*, 10: 318.

Del Campo, N., S. R. Chamberlain, B. J. Sahakian, and T. W. Robbins. 2011. 'The roles of dopamine and noradrenaline in the pathophysiology and treatment of attention-deficit/hyperactivity disorder', *Biol Psychiatry*, 69: e145-57.

Diallo, K., A. K. Oppong, and G. E. Lim. 2019. 'Can 14-3-3 proteins serve as therapeutic targets for the treatment of metabolic diseases?', *Pharmacol Res*, 139: 199-206.

Egan, R. J., C. L. Bergner, P. C. Hart, J. M. Cachat, P. R. Canavello, M. F. Elegante, S. I. Elkhayat, B. K. Bartels, A. K. Tien, D. H. Tien, S. Mohnot, E. Beeson, E. Glasgow, H. Amri, Z. Zukowska, and A. V. Kalueff. 2009. 'Understanding behavioral and physiological phenotypes of stress and anxiety in zebrafish', *Behav Brain Res*, 205: 38-44.

Favrot, L., A. E. Grzegorzewicz, D. H. Lajiness, R. K. Marvin, J. Boucau, D. Isailovic, M. Jackson, and D. R. Ronning. 2013. 'Mechanism of inhibition of Mycobacterium tuberculosis antigen 85 by ebselen', *Nat Commun*, 4: 2748.

Ghorbani, S., A. Fossbakk, A. Jorge-Finnigan, M. I. Flydal, J. Haavik, and R. Kleppe. 2016. 'Regulation of tyrosine hydroxylase is preserved across different homo- and heterodimeric 14-3-3 proteins', *Amino Acids*, 48: 1221-29.

Ghosh, A., B. N. Ratha, N. Gayen, K. H. Mroue, R. K. Kar, A. K. Mandal, and A. Bhunia. 2015. 'Biophysical Characterization of Essential Phosphorylation at the Flexible C-Terminal Region of C-Raf with 14-3-3ζ Protein', *PLoS One*, 10: e0135976.

Goins, C. M., S. Dajnowicz, S. Thanna, S. J. Sucheck, J. M. Parks, and D. R. Ronning. 2017. 'Exploring Covalent Allosteric Inhibition of Antigen 85C from Mycobacterium tuberculosis by Ebselen Derivatives', *ACS Infect Dis*, 3: 378-87.

Greco, T. M., R. Hodara, I. Parastatidis, H. F. Heijnen, M. K. Dennehy, D. C. Liebler, and H. Ischiropoulos. 2006. 'Identification of S-nitrosylation motifs by site-specific mapping of the S-

nitrosocysteine proteome in human vascular smooth muscle cells', *Proc Natl Acad Sci U S A*, 103: 7420-5.

Helander, L., A. Sharma, H. E. Krokan, K. Plaetzer, B. Krammer, N. Tortik, O. A. Gederaas, G. Slupphaug, and L. Hagen. 2016. 'Photodynamic treatment with hexyl-aminolevulinate mediates reversible thiol oxidation in core oxidative stress signaling proteins', *Mol Biosyst*, 12: 796-805.

Hermeking, H. 2003. 'The 14-3-3 cancer connection', *Nat Rev Cancer*, 3: 931-43.

Ichimura, T., T. Isobe, T. Okuyama, T. Yamauchi, and H. Fujisawa. 1987. 'Brain 14-3-3 protein is an activator protein that activates tryptophan 5-monooxygenase and tyrosine 3-monooxygenase in the presence of Ca2+,calmodulin-dependent protein kinase II', *FEBS Lett*, 219: 79-82.

Jacobsen, K. K., R. Kleppe, S. Johansson, T. Zayats, and J. Haavik. 2015. 'Epistatic and gene wide effects in YWHA and aromatic amino hydroxylase genes across ADHD and other common neuropsychiatric disorders: Association with YWHAE', *Am J Med Genet B Neuropsychiatr Genet*, 168: 423-32.

James, S. J., W. Slikker, S. Melnyk, E. New, M. Pogribna, and S. Jernigan. 2005. 'Thimerosal neurotoxicity is associated with glutathione depletion: Protection with glutathione precursors', *Neurotoxicology*, 26: 1-8.

Jandova, Z., Z. Trosanova, V. Weisova, C. Oostenbrink, and J. Hritz. 2018. 'Free energy calculations on the stability of the 14-3-3zeta protein', *Biochim Biophys Acta Proteins Proteom*, 1866: 442-50.

Jiang, H., Y. Yu, S. Liu, M. Zhu, X. Dong, J. Wu, Z. Zhang, M. Zhang, and Y. Zhang. 2019. 'Proteomic Study of a Parkinson's Disease Model of Undifferentiated SH-SY5Y Cells Induced by a Proteasome Inhibitor', *Int J Med Sci*, 16: 84-92.

Jin, Z., X. Du, Y. Xu, Y. Deng, M. Liu, Y. Zhao, B. Zhang, X. Li, L. Zhang, C. Peng, Y. Duan, J. Yu, L. Wang, K. Yang, F. Liu, R. Jiang, X. Yang, T. You, X. Liu, X. Yang, F. Bai, H. Liu, X. Liu, L. W. Guddat, W. Xu, G. Xiao, C. Qin, Z. Shi, H. Jiang, Z. Rao, and H. Yang. 2020. 'Structure of M(pro) from SARS-CoV-2 and discovery of its inhibitors', *Nature*, 582: 289-93.

Joice, A. C., M. T. Harris, E. W. Kahney, H. C. Dodson, A. G. Maselli, D. C. Whitehead, and J. C. Morris. 2013. 'Exploring the mode of action of ebselen in Trypanosoma brucei hexokinase inhibition', *Int J Parasitol Drugs Drug Resist*, 3: 154-60.

Kim, H. S., S. L. Ullevig, H. N. Nguyen, D. Vanegas, and R. Asmis. 2014. 'Redox regulation of 14-3-3ζ controls monocyte migration', *Arterioscler Thromb Vasc Biol*, 34: 1514-21.

Kleppe, R., S. Rosati, A. Jorge-Finnigan, S. Alvira, S. Ghorbani, J. Haavik, J. M. Valpuesta, A. J. R. Heck, and A. Martinez. 2014. 'Phosphorylation Dependence and Stoichiometry of the Complex Formed by Tyrosine Hydroxylase and 14-3-3 gamma', *Molecular & Cellular Proteomics*, 13: 2017-30.

Lass, A., P. Witting, R. Stocker, and H. Esterbauer. 1996. 'Inhibition of copper- and peroxyl radical-induced LDL lipid oxidation by ebselen: antioxidant actions in addition to hydroperoxide-reducing activity', *Biochim Biophys Acta*, 1303: 111-8.

Liao, W., S. Wang, C. Han, and Y. Zhang. 2005. '14-3-3 proteins regulate glycogen synthase 3beta phosphorylation and inhibit cardiomyocyte hypertrophy', *Febs j*, 272: 1845-54.

Lieberman, O. J., M. W. Orr, Y. Wang, and V. T. Lee. 2014. 'High-throughput screening using the differential radial capillary action of ligand assay identifies ebselen as an inhibitor of diguanylate cyclases', *ACS Chem Biol*, 9: 183-92.

Liu, M., X. Liu, P. Ren, J. Li, Y. Chai, S. J. Zheng, Y. Chen, Z. P. Duan, N. Li, and J. Y. Zhang. 2014. 'A cancer-related protein 14-3-3ζ is a potential tumor-associated antigen in immunodiagnosis of hepatocellular carcinoma', *Tumour Biol*, 35: 4247-56.

Masaki, C., A. L. Sharpley, C. M. Cooper, B. R. Godlewska, N. Singh, S. R. Vasudevan, C. J. Harmer, G. C. Churchill, T. Sharp, R. D. Rogers, and P. J. Cowen. 2016. 'Effects of the potential lithium-mimetic, ebselen, on impulsivity and emotional processing', *Psychopharmacology (Berl)*, 233: 2655-61.

Menendez, C. A., F. Bylehn, G. R. Perez-Lemus, W. Alvarado, and J. J. de Pablo. 2020. 'Molecular characterization of ebselen binding activity to SARS-CoV-2 main protease', *Sci Adv*, 6.

Mukherjee, S., W. S. Weiner, C. E. Schroeder, D. S. Simpson, A. M. Hanson, N. L. Sweeney, R. K. Marvin, J. Ndjomou, R. Kolli, D. Isailovic, F. J. Schoenen, and D. N. Frick. 2014. 'Ebselen inhibits hepatitis C virus NS3 helicase binding to nucleic acid and prevents viral replication', *ACS Chem Biol*, 9: 2393-403.

Nery, L. R., N. S. Eltz, L. Martins, L. D. Guerim, T. C. Pereira, M. R. Bogo, and M. R. Vianna. 2014. 'Sustained behavioral effects of lithium exposure during early development in zebrafish: involvement of the Wnt-beta-catenin signaling pathway', *Prog Neuropsychopharmacol Biol Psychiatry*, 55: 101-8.

Niesen, F. H., H. Berglund, and M. Vedadi. 2007. 'The use of differential scanning fluorimetry to detect ligand interactions that promote protein stability', *Nature Protocols*, 2: 2212-21.

Obsil, T., and V. Obsilova. 2011. 'Structural basis of 14-3-3 protein functions', *Semin Cell Dev Biol*, 22: 663-72.

Pagan, C., H. Goubran-Botros, R. Delorme, M. Benabou, N. Lemiere, K. Murray, F. Amsellem, J. Callebert, P. Chaste, S. Jamain, F. Fauchereau, G. Huguet, E. Maronde, M. Leboyer, J. M. Launay, and T. Bourgeron. 2017. 'Disruption of melatonin synthesis is associated with impaired 14-3-3 and miR-451 levels in patients with autism spectrum disorders', *Sci Rep*, 7: 2096.

Parran, D. K., A. Barker, and M. Ehrich. 2005. 'Effects of thimerosal on NGF signal transduction and cell death in neuroblastoma cells', *Toxicological Sciences*, 86: 132-40.

Pennington, K. L., T. Y. Chan, M. P. Torres, and J. L. Andersen. 2018. 'The dynamic and stress-adaptive signaling hub of 14-3-3: emerging mechanisms of regulation and context-dependent protein-protein interactions', *Oncogene*, 37: 5587-604.

Pozuelo Rubio, M., K. M. Geraghty, B. H. Wong, N. T. Wood, D. G. Campbell, N. Morrice, and C. Mackintosh. 2004. '14-3-3-affinity purification of over 200 human phosphoproteins reveals new links to regulation of cellular metabolism, proliferation and trafficking', *Biochem J*, 379: 395-408.

Ren, J., Y. Zhao, E. E. Fry, and D. I. Stuart. 2018. 'Target Identification and Mode of Action of Four Chemically Divergent Drugs against Ebolavirus Infection', *J Med Chem*, 61: 724-33.

Sies, H., and M. J. Parnham. 2020. 'Potential therapeutic use of ebselen for COVID-19 and other respiratory viral infections', *Free Radic Biol Med*, 156: 107-12.

Singh, N., A. C. Halliday, J. M. Thomas, O. V. Kuznetsova, R. Baldwin, E. C. Woon, P. K. Aley, I. Antoniadou, T. Sharp, S. R. Vasudevan, and G. C. Churchill. 2013. 'A safe lithium mimetic for bipolar disorder', *Nat Commun*, 4: 1332.

Singh, N., A. L. Sharpley, U. E. Emir, C. Masaki, M. M. Herzallah, M. A. Gluck, T. Sharp, C. J. Harmer, S. R. Vasudevan, P. J. Cowen, and G. C. Churchill. 2016. 'Effect of the Putative Lithium Mimetic Ebselen on Brain Myo-Inositol, Sleep, and Emotional Processing in Humans', *Neuropsychopharmacology*, 41: 1768-78.

Skjevik, A. A., M. Mileni, A. Baumann, O. Halskau, K. Teigen, R. C. Stevens, and A. Martinez. 2014. 'The N-Terminal Sequence of Tyrosine Hydroxylase Is a Conformationally Versatile Motif That Binds 14-3-3 Proteins and Membranes', *Journal of Molecular Biology*, 426: 150-68.

Stevers, L. M., E. Sijbesma, M. Botta, C. MacKintosh, T. Obsil, I. Landrieu, Y. Cau, A. J. Wilson, A. Karawajczyk, J. Eickhoff, J. Davis, M. Hann, G. O'Mahony, R. G. Doveston, L. Brunsveld, and C. Ottmann. 2018. 'Modulators of 14-3-3 Protein-Protein Interactions', *J Med Chem*, 61: 3755-78.

Sugden, P. H., S. J. Fuller, S. C. Weiss, and A. Clerk. 2008. 'Glycogen synthase kinase 3 (GSK3) in the heart: a point of integration in hypertrophic signalling and a therapeutic target? A critical analysis', *Br J Pharmacol*, 153 Suppl 1: S137-53.

Torrico, B., E. Anton-Galindo, N. Fernandez-Castillo, E. Rojo-Francas, S. Ghorbani, L. Pineda-Cirera, A. Hervas, I. Rueda, E. Moreno, J. M. Fullerton, V. Casado, J. K. Buitelaar, N. Rommelse, B. Franke, A. Reif, A. G. Chiocchetti, C. Freitag, R. Kleppe, J. Haavik, C. Toma, and B. Cormand.

26

2020. 'Involvement of the 14-3-3 Gene Family in Autism Spectrum Disorder and Schizophrenia: Genetics, Transcriptomics and Functional Analyses', *J Clin Med*, 9.

Urbaneja, M. A., L. Skjærven, O. Aubi, J. Underhaug, D. J. López, I. Arregi, M. Alonso-Mariño, A. Cuevas, J. A. Rodríguez, A. Martinez, and S. Bañuelos. 2017. 'Conformational stabilization as a strategy to prevent nucleophosmin mislocalization in leukemia', *Sci Rep*, 7: 13959.

Valenti, D., J. F. Neves, F. X. Cantrelle, S. Hristeva, D. Lentini Santo, T. Obšil, X. Hanoulle, L. M. Levy, D. Tzalis, I. Landrieu, and C. Ottmann. 2019. 'Set-up and screening of a fragment library targeting the 14-3-3 protein interface', *Medchemcomm*, 10: 1796-802.

van Heusden, G. P. H. 2005. '14-3-3 proteins: Regulators of numerous eukaryotic proteins', *Iubmb Life*, 57: 623-29.

Vaudel, M., J. M. Burkhart, R. P. Zahedi, E. Oveland, F. S. Berven, A. Sickmann, L. Martens, and H. Barsnes. 2015. 'PeptideShaker enables reanalysis of MS-derived proteomics data sets', *Nat Biotechnol*, 33: 22-4.

Vilchez, D., I. Saez, and A. Dillin. 2014. 'The role of protein clearance mechanisms in organismal ageing and age-related diseases', *Nat Commun*, 5: 5659.

Waloen, K., R. Kleppe, A. Martinez, and J. Haavik. 2017. 'Tyrosine and tryptophan hydroxylases as therapeutic targets in human disease', *Expert Opin Ther Targets*, 21: 167-80.

Wang, Y., J. Wallach, S. Duane, Y. Wang, J. Wu, J. Wang, A. Adejare, and H. Ma. 2017. 'Developing selective histone deacetylases (HDACs) inhibitors through ebselen and analogs', *Drug Des Devel Ther*, 11: 1369-82.

Woodcock, J. M., C. Coolen, K. L. Goodwin, D. J. Baek, R. Bittman, M. S. Samuel, S. M. Pitson, and A. F. Lopez. 2015. 'Destabilisation of dimeric 14-3-3 proteins as a novel approach to anti-cancer therapeutics', *Oncotarget*, 6: 14522-36.

Xiao, Y., V. Y. Lin, S. Ke, G. E. Lin, F. T. Lin, and W. C. Lin. 2014. '14-3-3tau promotes breast cancer invasion and metastasis by inhibiting RhoGDIalpha', *Mol Cell Biol*, 34: 2635-49.

Yang, X., W. H. Lee, F. Sobott, E. Papagrigoriou, C. V. Robinson, J. G. Grossmann, M. Sundström, D. A. Doyle, and J. M. Elkins. 2006. 'Structural basis for protein-protein interactions in the 14-3-3 protein family', *Proc Natl Acad Sci U S A*, 103: 17237-42.

FOOTNOTES

CONFLICT OF INTEREST

JH has received speaker honoraria from Lilly, Shire, HB Pharma, Medice, Takeda and Biocodex. No other conflict of interest.

STATEMENTS

This study has not been pre-registered. Custom-made materials will be shared upon reasonable request.

LEGENDS FOR FIGURES

Figure 1. Screening of drugs interacting with 14-3-3ζ, and the destabilization caused by ebselen. (A) The 3D structure of dimeric 14-3-3ζ (PDB ID 1A4O) in ribbon and transparent surface representation. Cysteine residues are colored yellow. C25 and C189 are surface accessible, C94 is embedded within the protein. (B) DSF-based screening of 14-3-3ζ with the Prestwick Chemical Library (1280 compounds). All T_m-values obtained are represented, blue dots indicate the compounds that provide a T_m-value for 14-3-3ζ within 10xSD of the 4% DMSO control (T_m = 61.1 ± 0.5°C), and green dots indicate primary hits, all causing a decrease in the T_m of 14-3-3ζ below 56.1°C (Table S1). Best hits Ebselen and Thimerosal, which show consistent DSF-monitored concentration-dependent effect, are specifically marked (insets). AU, arbitrary fluorescence units. (C) Concentration dependent DSF for the effect of ebselen (0-5 μM) on the thermal stability of 14-3-3ζ (n=3; independent DSF measurements). (D) CD spectra of ebselen treated (blue) and untreated 14-3-3ζ (red). See Materials and methods for details on data analysis.

Figure 2. Covalent bonding of ebselen to 14-3-3ζ and identification of interacting cysteine residues. (A) SPR sensorgram is presented for the interaction of ebselen with immobilized 14-3-3ζ. The concentrations of ebselen added ranged from 0to 200 μM. (B) Positive ion CID MS/MS mass spectrum of ebselen (m/z = 275 Da) and ebselenated peptide containing C94 [DIC*NDVLSLLEK + 2H]$^{2+}$ (m/z: 818.85). The asterisk denotes one ebselen tag on the peptide cysteine group (m/z is ratio of mass/charge). (C) MALDI-TOF mass spectometry of C25A-C189A-14-3-3ζ mutant after ebselen treatment. Inset, the mayor peak corresponds to unlabelled mutant (theoretical m/z = 28005 Da), the following peak most probably represents an adduct with the MALDI matrix (ferulic acid, m/z = 180 Da) and ebselen-tagged protein (m/z≈ 28270), which presented low intensity. (D) MALDI-TOF mass spectrometry of C94A-14-3-3ζ mutant tagged with ebselen (see also Figure S2A). Inset, the first peak corresponds to unlabelled mutant (theoretical m/z = 28038 Da) and the following peaks to single and double-tagged proteins (see also Figure S2B).

Figure 3. The effect of ebselen modification on the kinetic stability and binding partner ability of 14-3-3ζ, and on the 14-3-3 levels in SHSY5Y cells. (A) The kinetic stability of ebselen-treated (black curve) and untreated 14-3-3ζ (red curve) measured by monitoring the time dependent increase of SYPRO Orange fluorescence at 37 °C up to 17 h, represented as the average of triplicate measurements at each time point, with SD in gray. AU, arbitrary fluorescence units. (B) SPR results (recorded response units (RU)) for the binding of pSer19TH to immobilized 14-3-3ζ, either untreated (red bars) or treated with ebselen (black bars), measured at two concentrations of pSer19TH. Data represent the average

29

(± SD) of duplicate measurements with two different preparations of pSer19TH. (C) Concentration dependent DSF results comparing the melting points of 14-3-3ζ (red), γ (green), and ε (blue) following treatment with ebselen. (D) shows the effect of 14-3-3γ, ebselen treated 14-3-3 (Eb 14-3-3) and ebselen oxide treated 14-3-3 (Eb ox 14-3-3) on pSer19TH dephosphorylation. The inset shows the remaining [^{32}P]-pSer19 at different time points for samples run in absence of phosphatase (●, dotted line), in the presence of phosphatase, but no 14-3-3 (○), 14-3-3 control (□), ebselen treated 14-3-3 (■) and ebselen oxide treated 14-3-3 (▲). The bar plot shows the remaining [^{32}P]-pSer19 (in %, relative to samples with no phosphatase added) after 10 min reaction, shown as mean + ST.DEV. (n=3). P-values (t-test, two-sided, different variance) of 0.013 (*) and 1.55 10^{-6} (**), were calculated for 14-3-3 control (Ctr. 14-3-3) compared to ebselen- or ebselen oxide treated 14-3-3, respectively.

Figure 4. (A) Immunofluorescence investigation of neuroblastoma cells: untreated and ebselen treated (5 µM in 0.05% DMSO). A DMSO control (0.05%) is also shown. Pan 14-3-3 (green) and -actin (red) were immunodetected. Nuclei were stained with DAPI. Scale bars, 10 µm. (B) Western blot investigation using SHSY5Y cell samples untreated and treated with ebselen as in (A); 14-3-3 was immunodetected using actin as a loading control. Densitometric analysis was carried out to perform the statistical analysis, showing the reduction of 14-3-3 level in ebselen treated cells compared with untreated (DMSO control arbitrarily taken as 1) (n=4, independent cell culture preparations, p=0.004). (C) Western blot of SHSY5Y cells comparing pan 14-3-3 levels upon treatment with 500 nM Bortezomib, 10 µM ebselen and 50 µM Z-VAD-FMK. GAPDH was used as a loading reference. Densitometric analysis was used to determine the comparison of the treated samples with the untreated (arbitrarily taken as 1) (n=3, independent cell culture preparations; p<0.05). Statistical analyses by 2-tailed Student's t test (B), and one-way ANOVA with the Holm-Sidak method (C). (*) p< 0.5, (**) p < 0.005, (***) p < 0.001. All data are presented as mean ± SD.

Figure 5. Effects of ebselen and ebselen oxide on 14-3-3 levels in SHSY5Y cells. (A) Cells were treated with increasing concentrations of ebselen or ebselen oxide showing the reduction of 14-3-3ζ level with increasing concentration of the respective compounds, compared with untreated (DMSO control). (B) Western blot of SHSY5Y cells comparing total 14-3-3 levels upon treatment with 500 nM Bortezomib, 5 µM ebselen oxide showing the reduction of 14-3-3ζ level with ebselen oxide compared with proteasomal inhibitor treated cells in presence of ebselen oxide. GAPDH was used as a loading reference. Densitometric analysis was used to determine the comparison of the treated samples with the untreated (arbitrarily taken as 1) (n=5, independent cell culture preparations; p<0.05). Statistical analyses by 2-tailed Student's t test. (*) p< 0.05. All data are presented as mean ± SD.

Figure 6. Effect of ebselen on 14-3-3 abundance in the zebrafish brain and on behavior. (A) Western blot of WT zebrafish brain lysate for DMSO control (0,01%) and ebselen treated animals (1 µM in 0.01% DMSO). 14-3-3 was immunodetected in the samples with GAPDH as loading control. Densitometric analysis was used to determine the reduction of 14-3-3 abundance in ebselen treated zebrafish (n 3, independent lysates of 1 zebrafish each, *p<0.05). (B) Tanks used to measure visually-mediated social preference. (C) Visually-mediated social preference: WT zebrafish spend more time freezing following ebselen treatment compared to DMSO-treated controls (p 0.0003). (D) Visually-mediated social preference: ebselen treated zebrafish swim significantly less (p < 0.0001). Unpaired t-test with Welch's correction or Mann-Whitney U test. (E) Tank used in the novel tank test. (F) Freezing behaviour is not affected by ebselen treatment in the novel tank test (p = 0.22). (G) Locomotion is not affected by ebselen treatment in the novel tank test (p = 0.18)). Unpaired t-test with Welch's correction or Mann-Whitney U test. (H) Tank used in the open field test. (I) Freezing behaviour is not affected by ebselen treatment in the open field test (p = 0.68). (J) Locomotion is not affected by ebselen treatment in the open field test (p = 0.67). For C,D) n = 10 DMSO controls, and n=12 for ebselen treated animals; for F,G,l,J) . Unpaired t-test with Welch's correction. (***) p < 0.001, (****) p < 0.0001. Mean ± SEM.

TABLES

Table 1. Effect of ebselen on the midpoint melting temperatures (T_m) of 14-3-3ζ (wild-type and cysteine mutants)

14-3-3ζ-	T_m (- Ebselen) (°C)	T_m (+ Ebselen) (°C)	ΔT_m (+ Ebselen) - (-Ebselen) (°C)
Wild-type	60.1 ± 1.3	53.1 ± 1.3	-7.0 ± 1.3
C25A	59.9 ± 0.1 (-0.2 ± 0.6)*	50.9 ± 0.8	-9.0 ± 0.9
C25A-C94A	56.3 ± 0.4 (-4.8 ± 0.5)	53.5 ± 0.8	-2.8 ± 1.2
C25A-C189A	59.2 ± 0.3 (-0.7 ± 0.8)	50.6 ± 0.6	-8.6 ± 0.9
C25A-C94I-C189A	57.9 ± 0.3 (-3.2 ± 0.8)	57.6 ± 0.1	-0.3 ± 0.4
C25A-C94V-C189A	57.3 ± 0.4 (-3.8 ± 0.9)	56.9 ± 0.1	-0.4 ± 0.5
C94A	56.3 ± 0.1 (-4.8 ± 0.6)	55.5 ± 1.1	-0.8 ± 1.2
C94A-C189A	55.2 ± 0.3 (-5.9 ± 0.8)	56.5 ± 1.7	-1.3 ± 2.0

*In parenthesis, the difference between T_m-values for non-treated (- Ebselen) mutants of 14-3-3ζ and wild-type 14-3-3ζ

Figure 1.   Mol. Pharm. #MOLPHARM-AR-2020-000184

Figure 1
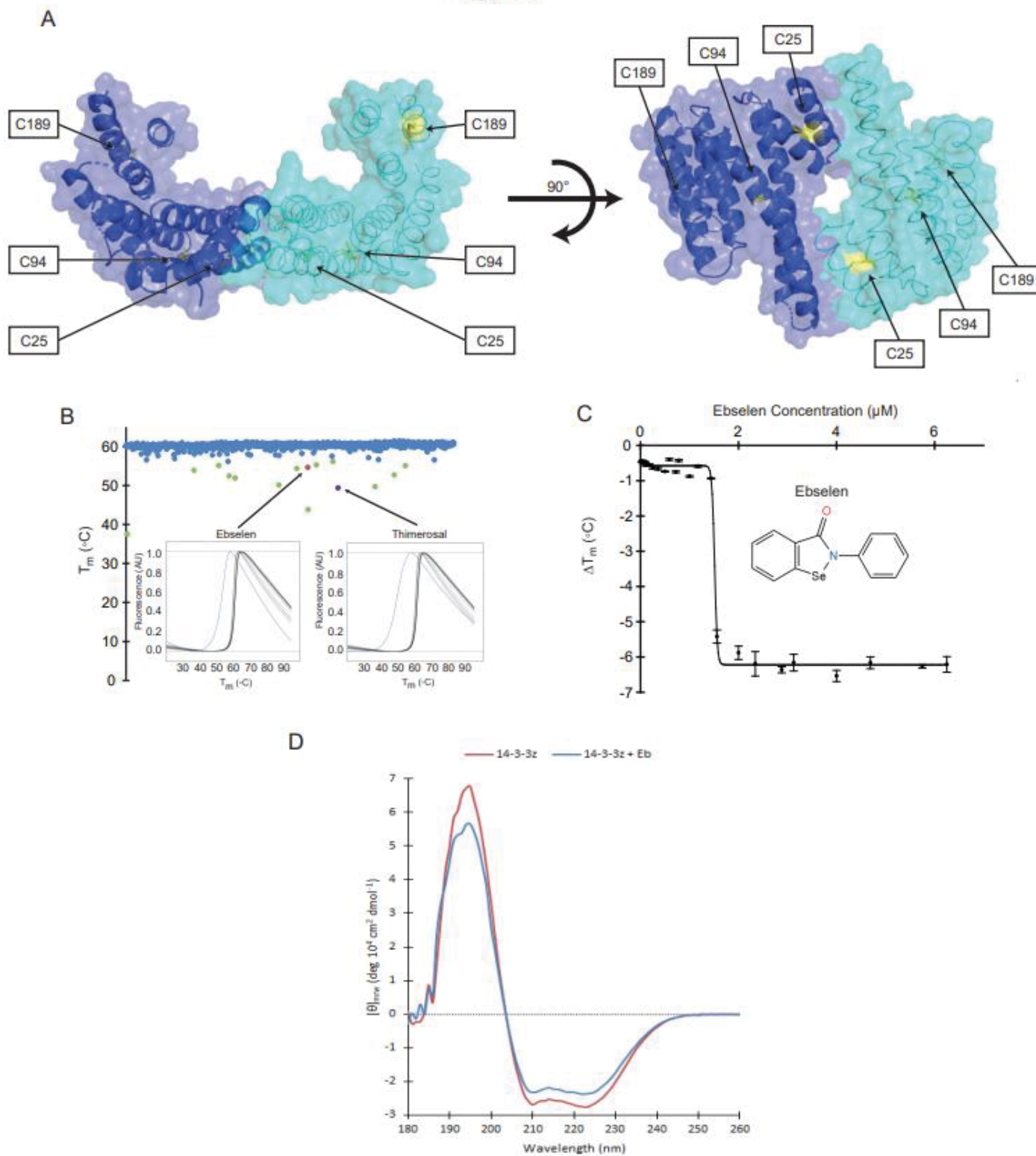
Figure 2.   Mol. Pharm. #MOLPHARM-AR-2020-000184
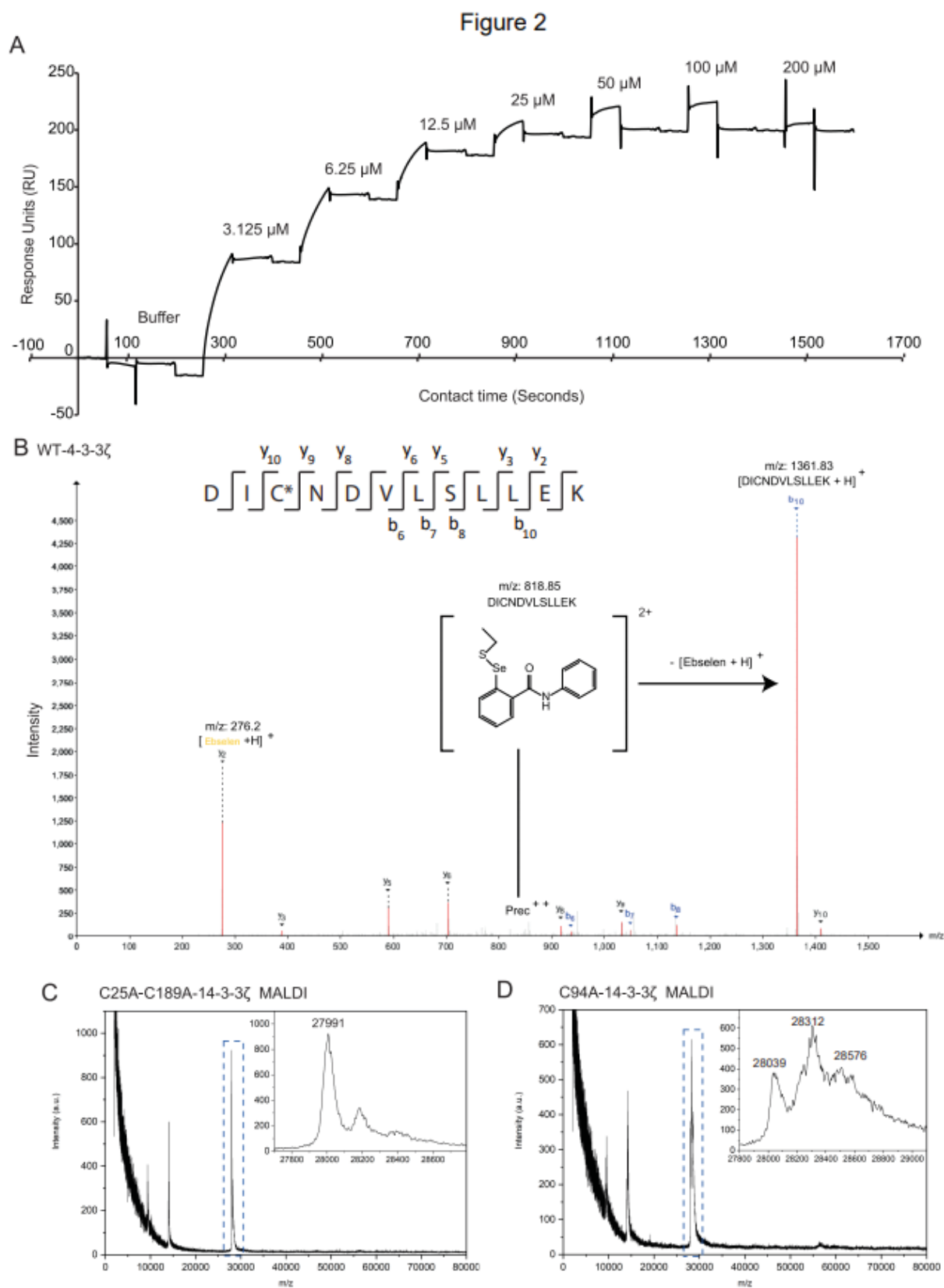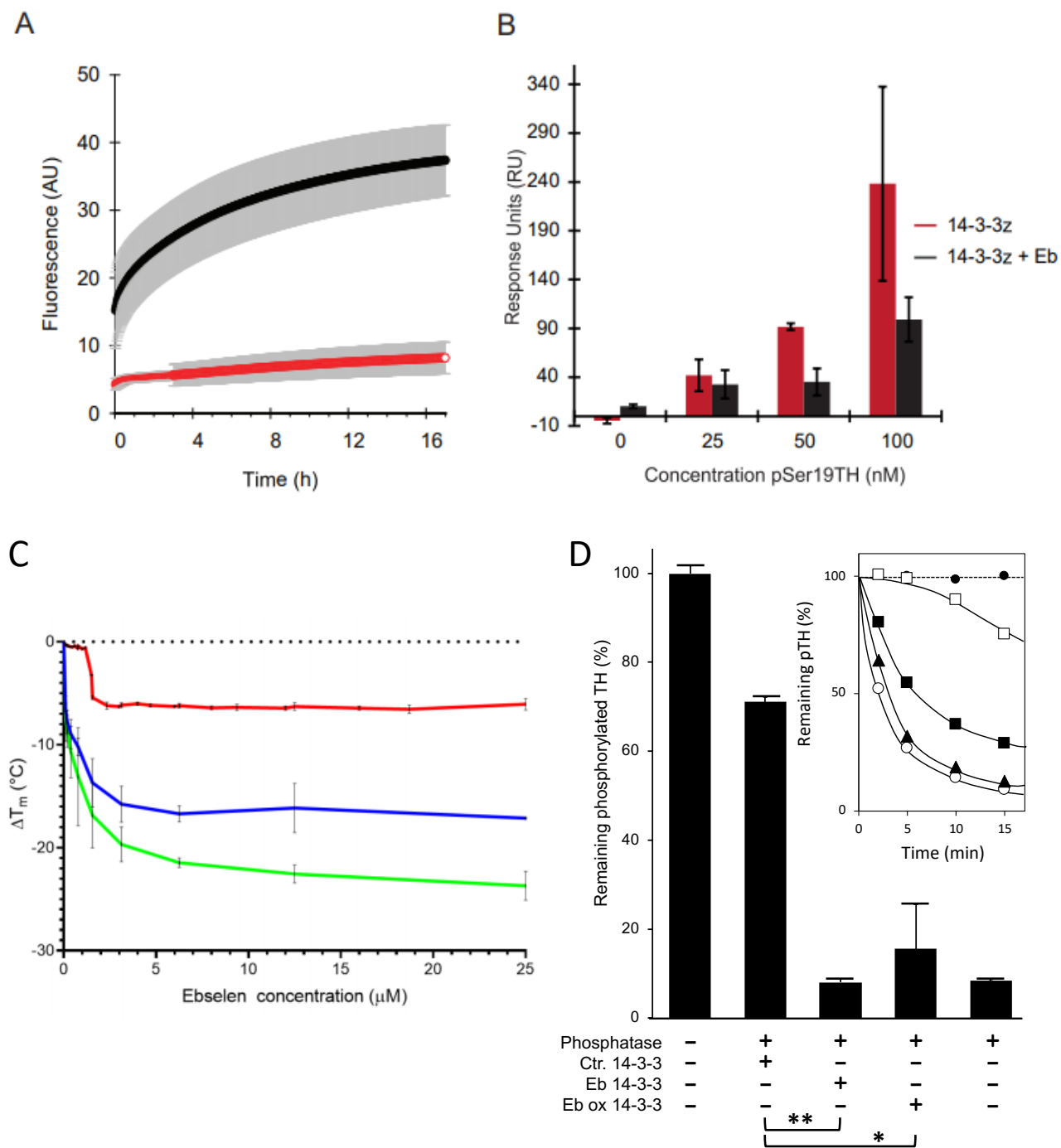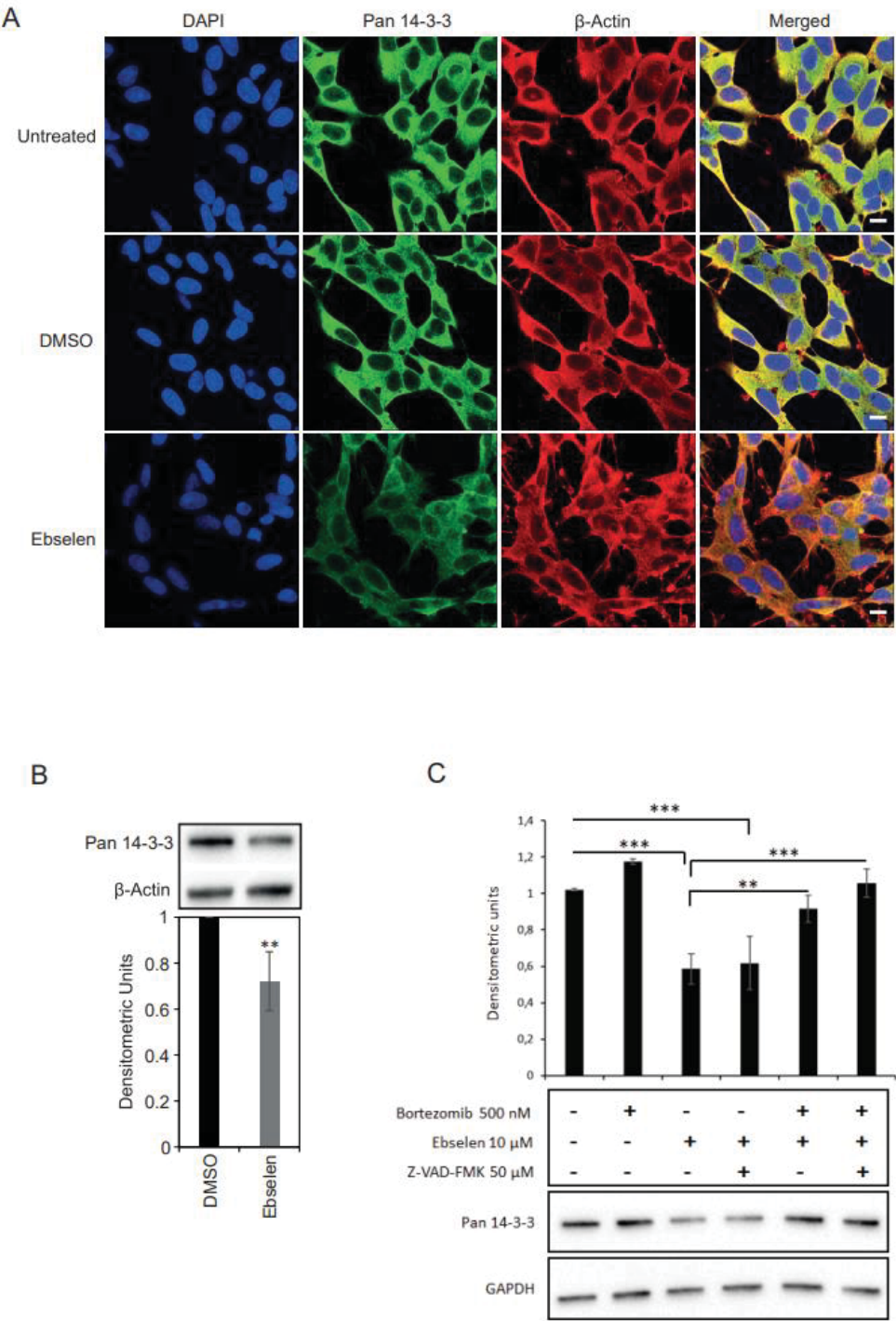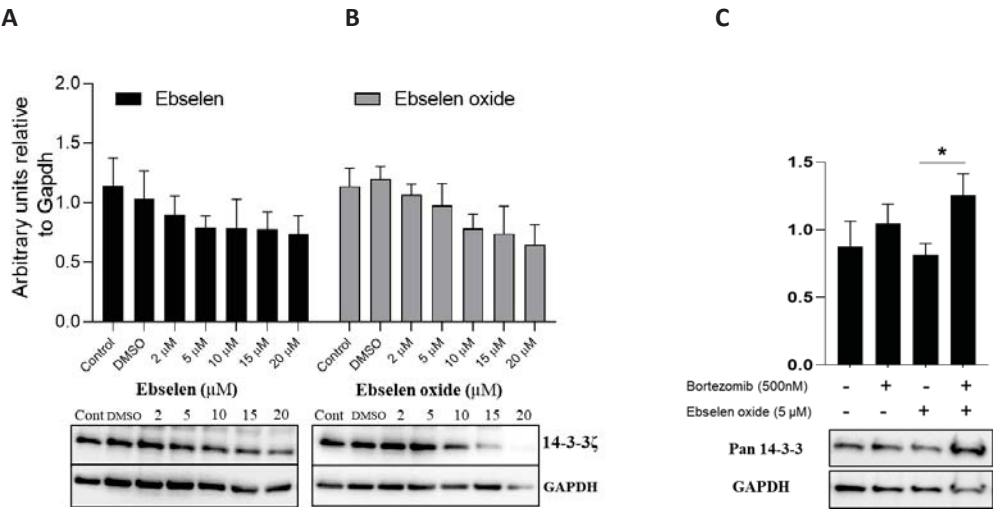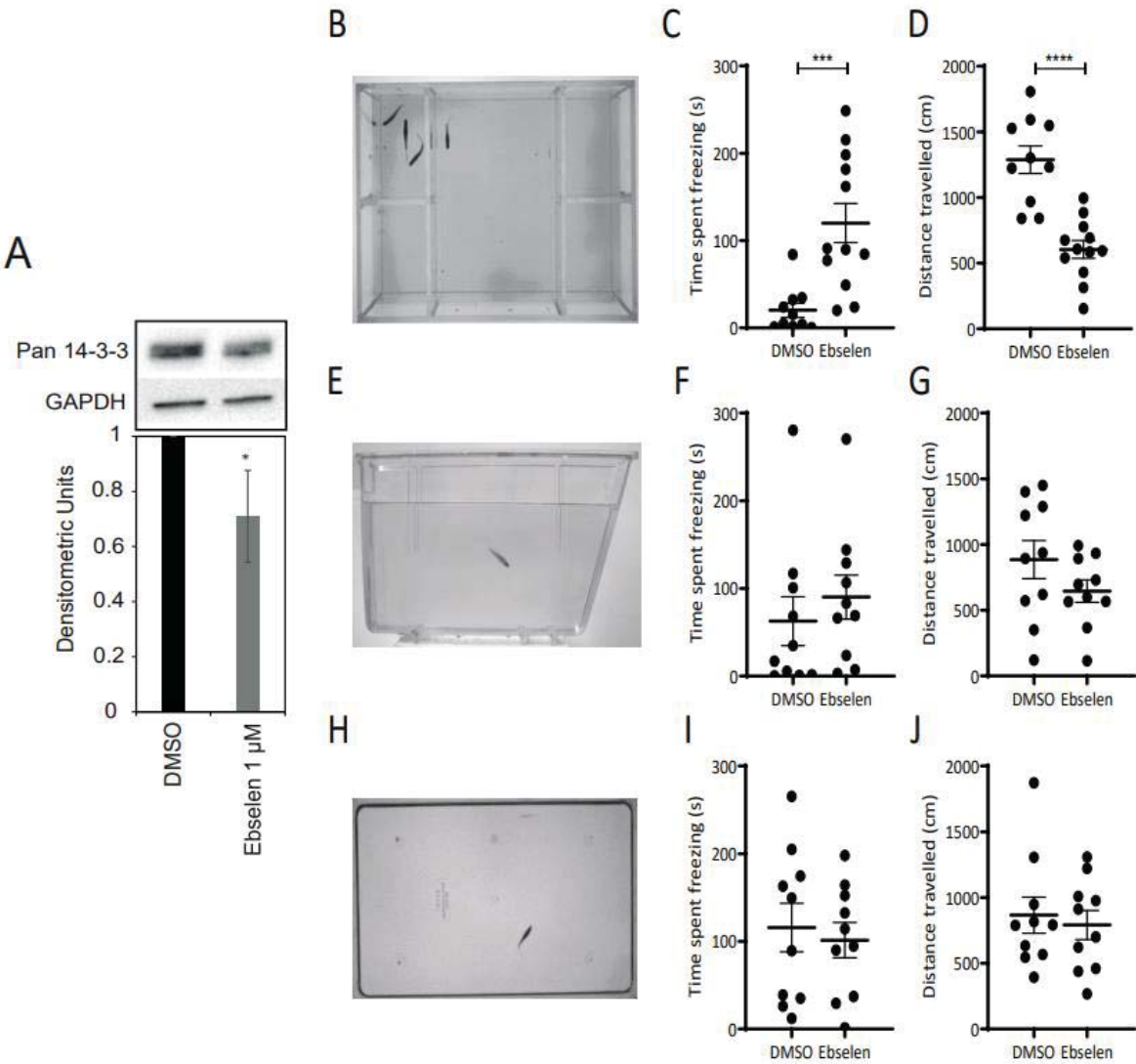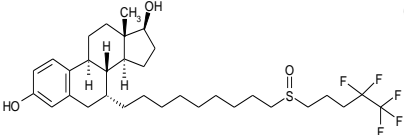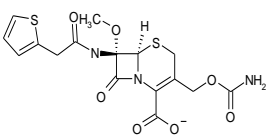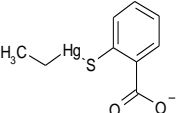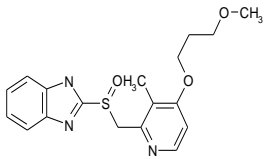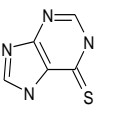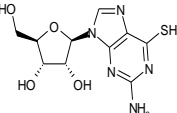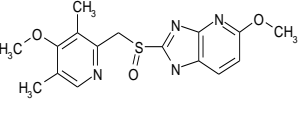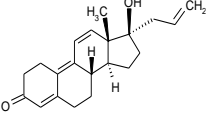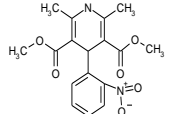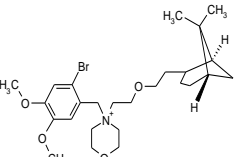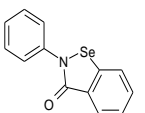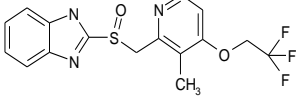
Figure 2

Figure 3

Figure 4.   Mol. Pharm. #MOLPHARM-AR-2020-000184

Figure 4

Fig. 5

A

B

C

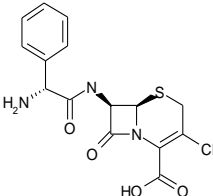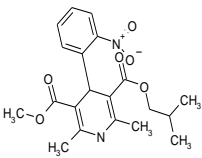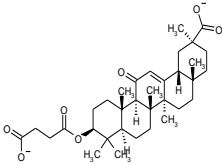Figure 6. revised   Mol. Pharm. #MOLPHARM-AR-2020-000184

Figure 5

Cysteine modification by ebselen reduces the stability and cellular levels of 14-3-3 proteins

Kai Waløen, Jung K.C. Kunwar, Elisa D. Vecchia, Sunil Pandey, Norbert Gasparik, Anne Døskeland, Sudarshan Patil, Rune Kleppe, Jozef Hritz, William H.J. Norton, Aurora Martinez, and Jan Haavik

ID	Drug name	Formula	Therapeutic class/ therapeutic effect	ΔT_m at 400 µM (°C)
1	Fulvestrant*		Endocrinology/ Antineoplastic	-23.6
2	Cefoxitin		Metabolism/ Antibacterial	-17.3
3	Thimerosal		Infectiology/ Antiseptic	-11.7
4	Rabeprazole[1]		Metabolism/ Antiulcer	-11.4
5	Mercaptopurine		Immunology/ Immunosuppressant	-10.8
6	Thioguanosine		Metabolism/ Antineoplastic	-9.2
7	Tenatoprazole[1]		Metabolism/ Antiulcer	-8.6
8	Altrenogest*		Endocrinology/ Progestogen	-8.4
9	Nifedipine[2]		Cardiovascular/ Antianginal	-7.2
10	Pinaverium[2]		Neuromuscular/ Antispastic	-6.7
11	Ebselen		Metabolism/ Anti-inflammatory	-7.0

12	Lansoprazole[1]		Metabolism/ Antiulcer	-6.0
13	Cefaclor		Infectiology/ Antibacterial	-6.0
14	Nisoldipine[2]		Cardiovascular/ Antianginal	-5.8
15	Carbenoxolone*,[3]		Metabolism/ Antiulcer	-5.1

Supplemental Table 1. Small-molecule drug hits obtained from the primary DSF screen. The midpoint melting temperature (T_m) of 14-3-3ζ with 4% DMSO was 61.1 ± 0.5°C, and 15 hits that caused $|\Delta T_m| \geq 10 \times SD$ (5.1°C), used as a cut-off value, were selected for concentration dependent studies. Based on its consistent concentration-dependent effect and reduced toxicity, ebselen was selected for further studies. *Steroids. [1]Proton pump inhibitor. [2]Calcium channel blocker [3]Probable calcium channel blocker

```
       1 [                    .         .         .         .         .          . 80
1 epsilon  -MDDREDLVYQAKLAEQAERYDEMVESMKKVAGMDVELTVEERNLLSVAYKNVIGARRASWRIISSIEQKEENKGGEDKL
2 sigma    --MERASLIQKAKLAEQAERYEDMAAFMKGAVEKGEELSCEERNLLSVAYKNVVGGQRAAWRVLSSIEQKSNEEGSEEKG
3 gamma    -MVDREQLVQKARLAEQAERYDDMAAAMKNVTELNEPLSNEERNLLSVAYKNVVGARRSSWRVISSIEQKTSADGNEKKI
4 eta      -MGDREQLLQRARLAEQAERYDDMASAMKAVTELNEPLSNEDRNLLSVAYKNVVGARRSSWRVISSIEQKTMADGNEKKL
5 theta    --MEKTELIQKAKLAEQAERYDDMATCMKAVTEQGAELSNEERNLLSVAYKNVVGGRRSAWRVISSIEQKT--DTSDKKL
6 beta     MTMDKSELVQKAKLAEQAERYDDMAAAMKAVTEQGHELSNEERNLLSVAYKNVVGARRSSWRVISSIEQKT--ERNEKKQ
7 zeta     --MDKNELVQKAKLAEQAERYDDMAACMKSVTEQGAELSNEERNLLSVAYKNVVGARRSSWRVVSSIEQKT--EGAEKKQ

       1                        .    1    .         .         .         .          : 160
1 epsilon  KMIREYRQMVETELKLICCDILDVLDKHLIPAAN--TGESKVFYYKMKGDYHRYLAEFATGNDRKEAAENSLVAYKAASD
2 sigma    PEVREYREKVETELQGVCDTVLGLLDSHLIKEAG--DAESRVFYLKMKGDYYRYLAEVATGDDKKRIIDSARSAYQEAMD
3 gamma    EMVRAYREKIEKELEAVCQDVLSLLDNYLIKNCSETQYESKVFYLKMKGDYYRYLAEVATGEKRATVVESSEKAYSEAHE
4 eta      EKVKAYREKIEKELETVCNDVLSLLDKFLIKNCNDFQYESKVFYLKMKGDYYRYLAEVASGEKKNSVVEASEAAYKEAFE
5 theta    QLIKDYREKVESELRSICTTVLELLDKYLIANAT--NPESKVFYLKMKGDYFRYLAEVACGDDRKQTIDNSQGAYQEAFD
6 beta     QMGKEYREKIEAELQDICNDVLELLDKYLIPNAT--QPESKVFYLKMKGDYFRYLSEVASGDNKQTTVSNSQQAYQEAFE
7 zeta     QMAREYREKIETELRDICNDVLSLLEKFLIPNAS--QAESKVFYLKMKGDYYRYLAEVAAGDDKKGIVDQSQQAYQEAFE

       1                   .         .         .         2         .         .          . 240
1 epsilon  IAMTELPPTHPIRLGLALNFSVFYYEILNSPDRACRLAKAAFDDAIAELDTLSEESYKDSTLIMQLLRDNLTLWTSDMQG
2 sigma    ISKKEMPPTNPIRLGLALNFSVPHYEIANSPEEAISLAKTTFDEAMADLHTLSEDSYKDSTLIMQLLRDNLTLWTADNAG
3 gamma    ISKEHMQPTHPIRLGLALNYSVFYYEIQNAPEQACHLAKTAFDDAIAELDTLNEDSYKDSTLIMQLLRDNLTLWTSDQQD
4 eta      ISKEQMQPTHPIRLGLALNFSVFYYEIQNAPEQACLLAKQAFDDAIAELDTLNEDSYKDSTLIMQLLRDNLTLWTSDQQD
5 theta    ISKKEMQPTHPIRLGLALNFSVFYYEILNNPELACTLAKTAFDEAIAELDTLNEDSYKDSTLIMQLLRDNLTLWTSDSAG
6 beta     ISKKEMQPTHPIRLGLALNFSVFYYEILNSPEKACSLAKTAFDEAIAELDTLNEESYKDSTLIMQLLRDNLTLWTSENQG
7 zeta     ISKKEMQPTHPIRLGLALNFSVFYYEILNSPEKACSLAKTAFDEAIAELDTLSEESYKDSTLIMQLLRDNLTLWTSDTQG

       1              :          ] 258
1 epsilon  DGEEQNKEALQDVEDENQ
2 sigma    EEGGEAPQEPQS------
3 gamma    DDGGEGNN----------
4 eta      EEAGEGN-----------
5 theta    EECDAAEGAEN-------
6 beta     DEGDAGEGEN----+---
7 zeta     DEAEAGEGGEN-------
```
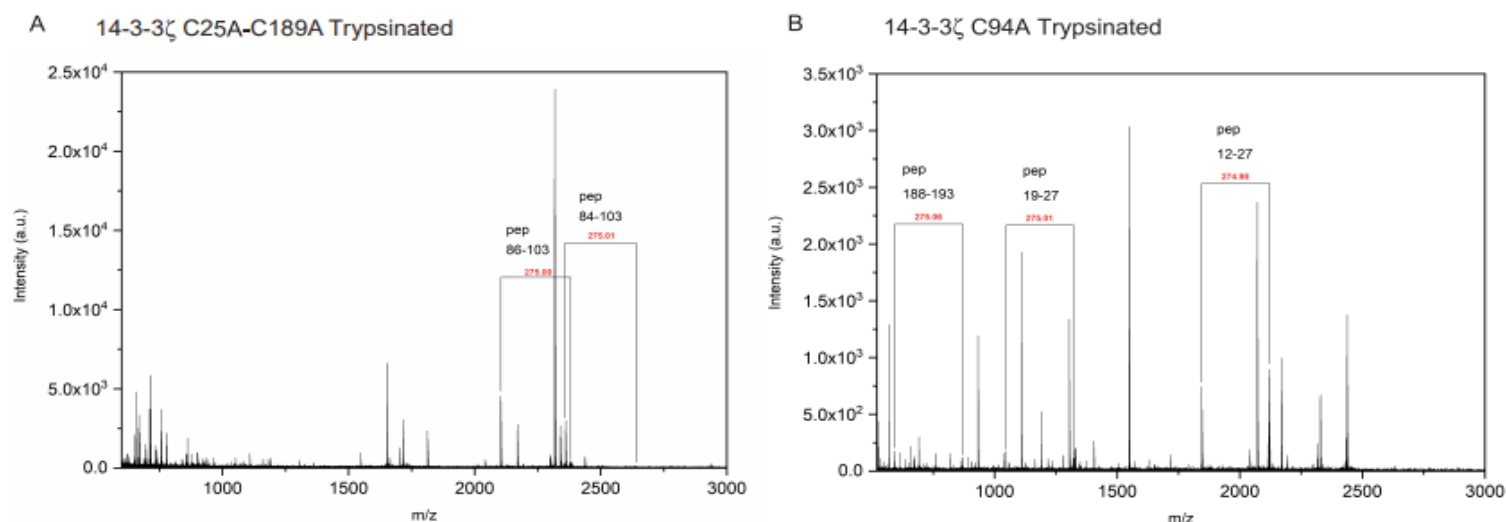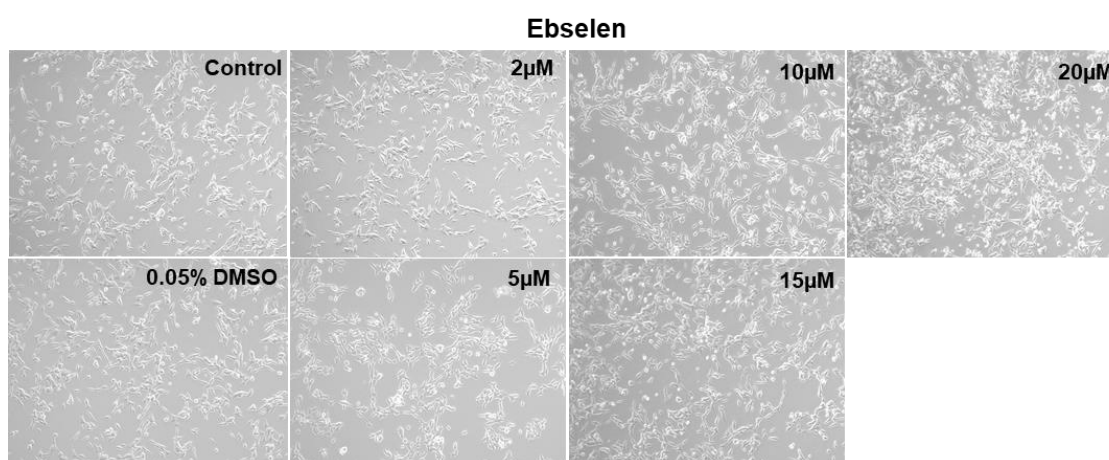
Supplemental Figure S1. Amino acid sequences of the seven isoforms of 14-3-3 are presented. The cysteine residues are highlighted in yellow.

A 14-3-3ζ C25A-C189A Trypsinated

B 14-3-3ζ C94A Trypsinated

pep 86-103   275.00

pep 84-103   275.01

pep 188-193   275.00

pep 19-27   275.01
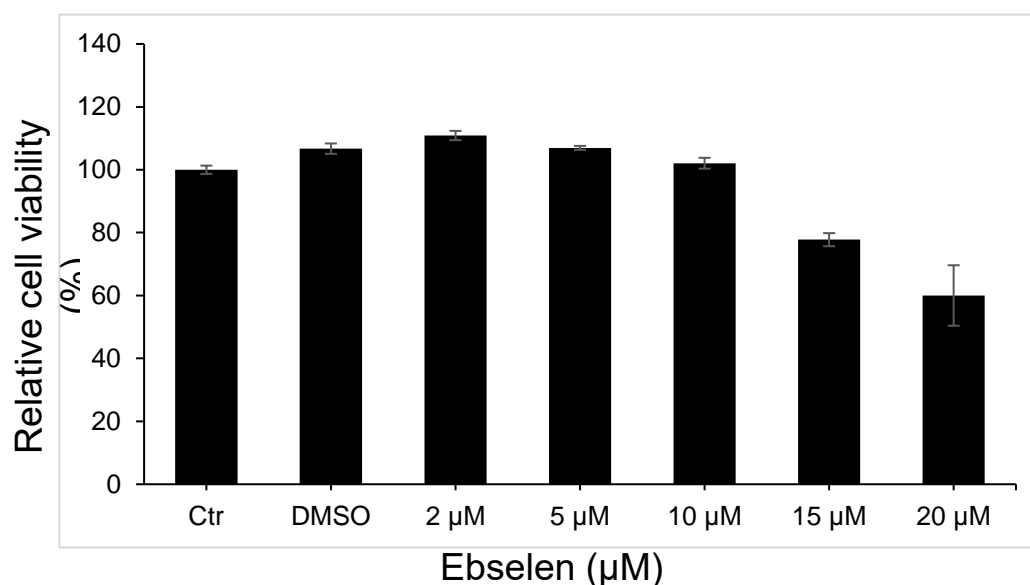
pep 12-27   274.98

Supplemental Figure S2. MALDI-TOF MS/MS peptide analysis of trypsin digested 1433ζ mutant constructs. a) 1433ζ-C25A-C189A and b) 1433ζ-C94A, after ebselen treatment. Peptides containing cysteines in tagged and untagged form (peptides with a mass shift of 275 Da) are denoted. In a) the figure shows two peptides involving ebselen tagging of C94 in very small amounts. In b) the figure shows a peptide involving C189 and two peptides involving C25.

4

Supplementary Figure S3. Viability of SHSY5Y cells treated with increasing concentration of ebselen and ebselen oxide. A Cell Titer-Blue assay was performed to examine cell viability of SHSY5Y cells treated with increasing concentration of ebselen and ebselen oxide. The cells were plated in 96-well plates at the density of 25000 cells per well and 5 h later were treated with different concentration of ebselen, ebselen oxide and DMSO (0.05%). Cells were then incubated for 16 h and then 20 μL of Cell Titre Blue reagent was added to each well. The plates were incubated for 2hrs before the fluorescence (λ=590) was measured with Victor 3 1420 Multilabel counter plate reader. A, Cell images using ebselen, B, relative cell viability using ebselen, C Cell images using ebselen oxide D, relative cell viability with ebselen oxide. Statistical analyses by 2-tailed Student's t test. (*) $p < 0.05$, (**) $p < 0.005$, (***) $p < 0.001$, (****) $p < 0.0001$. All data are presented as mean ± SEM.
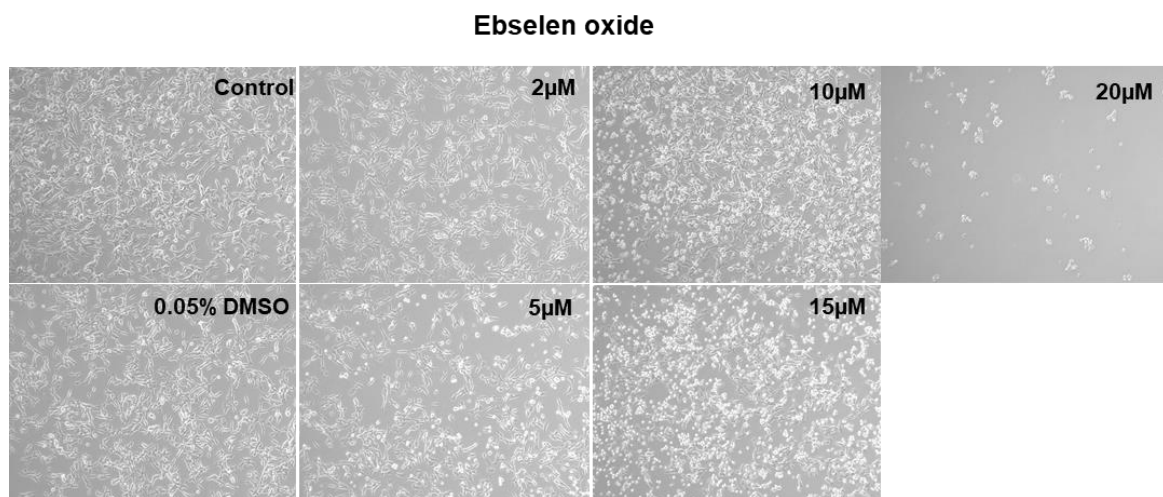
A

B

C

Ebselen oxide

D